

# UNIVERSITÀ DEGLI STUDI DI PADOVA

**Dipartimento di Fisica e Astronomia "Galileo Galilei"**

**Corso di Laurea in Fisica**


**Tesi di Laurea**

## Il modello cosmologico standard e la tensione di Hubble

## The standard cosmological model and the Hubble tension


**Relatore**

**Prof. Marco Peloso**

**Laureando**

**Matteo Barbon**


**Anno Accademico 2022/2023**

**Sommario**

L'attuale velocità di espansione dell'universo è parametrizzata dalla costante di Hubble. Questa quantità può essere determinata sia "localmente", attraverso misurazioni di redshift e distanza di eventi nell'universo recente (come le supernove), sia "globalmente", dalla storia del modello cosmologico che si può dedurre dai dati della radiazione cosmica di fondo (CMB). Questi due metodi conducono a risultati diversi di circa 5 sigma. L'obbiettivo di questa tesi è quello di studiare i principi teorici e le quantità fisiche alla base delle due misurazioni. Riguardo la misura locale, esaminiamo il modello cosmologico standard e i concetti di distanza e di redshift usati nel diagramma di Hubble. Riguardo la misura globale, studiamo come le perturbazioni cosmologiche si sono generate durante l'inflazione, come esse si manifestano nelle anisotropie della CMB e come la CMB può essere usata per dedurre i parametri cosmologici, tra cui la costante di Hubble.

**Abstract**

The current expansion rate of the universe is parameterized by the Hubble constant. This quantity can be measured either "locally", from the redshift-distance measurements of events in the late universe (such as supernovae) or "globally", from the integrated cosmological history that can be inferred from the Cosmic Microwave Background (CMB) radiation data. These two methods lead to different results at approximately the 5 sigma level. The goal of the thesis is to review the theoretical framework and the physical quantities at the basis of the two measurements. Concerning the local measurement, we review the standard cosmological model and the concept of luminosity distance and redshift used in the so called Hubble diagrams. Concerning the global measurement, we study how cosmological perturbations are generated during inflation, how they imprint the CMB anisotropies, and how the CMB can be used to infer cosmological parameters such as the Hubble constant.

# Contents

# 1 Introduction

The best-fitting theory for describing the statistics of the universe on large scales is known as the standard cosmological model. It is commonly referred to as $\Lambda$ cold dark matter ($\Lambda$CDM) model since it is a model in which the matter is mostly cold and dark (namely collisionless and with no electromagnetic interactions), and in which the current majority of the universe energy density behaves like vacuum energy (or cosmological constant) which drives the current accelerated expansion of the universe observed for the first time in 1998 (see refs. [10] and [20]). It provides a good agreement with the datasets currently available just exploiting six free-parameters (usually: Hubble constant $H_0$, baryon fractional density $\Omega_b$, matter fractional density $\Omega_m$, curvature fluctuation amplitude $A_s$, scalar spectral index $n_s$, optical depth $\tau$). One of the most significant successes of the model is the prediction of the existence and structure of the cosmic microwave background (CMB), moreover the CMB temperature and polarization measurements can be used to compare the $\Lambda$CDM model against data and provide an estimation of the six parameters [7]. The numerous successes of the $\Lambda$CDM model, along with technological advancements that allow for increasingly accurate measurements, motivate progressively in-depth studies. On one hand the $\Lambda$CDM contains vast areas of ignorance especially regarding inflation, dark matter and dark energy, on the other hand some tensions have emerged between recent observations and $\Lambda$CDM model predictions (for example the $\sim 5\sigma$ Hubble tension [1] and the $\sim 5\sigma$ CMB dipole tension [21]). For these reasons there is currently active research into many aspects of the $\Lambda$CDM model.
The Hubble tension, that we mentioned above, is widely acknowledged as one of the most urgent problem in the current cosmology. It concerns the discrepancy ($\sim 5\sigma$) between the two currently most accredited measurements of the Hubble constant $H_0$. The first one (early measurement) is provided by the Planck collaboration and it is based on the CMB measurement of Planck spacecraft ($H_0 = 67.4 \pm 0.5 \frac{\text{km}}{\text{sec Mpc}}$, [7]), the second one (late measurement), instead, is given by SH0ES (Supernovae, $H_0$, for the Equation of State of dark energy) project (started in 2005) through measuring the distance-redshift relation of nearby celestial bodies ($z < 1$) such as supernovae ($H_0 = 73.2 \pm 1.3 \frac{\text{km}}{\text{sec Mpc}}$, [8]). Since the estimate provided by the Planck collaboration heavily relies on the entire history of the cosmological model unlike the other one which depends only on recent cosmology, if the origin of the tension can not be attributed to a systematic error, then this would be the evidence of new physics beyond the current cosmological model. For this reason numerous researchers are attempting to modify the $\Lambda$CDM model in order to resolve or alleviate the various tensions (for example, by adding an early dark energy component or modifying the theory of gravity, [1]).
The aim of this thesis is to describe the theoretical framework underlying the two different measurements of the Hubble constant. At the beginning, we will present the aspects of the cosmological model that will be necessary for this purpose, initially studying the uniform background of the universe (its geometry and composition) and then introducing inhomogeneities in it (perturbing the metric, the stress-energy-momentum tensor, and the Einstein equations at first order). Subsequently, regarding the "Late measurement", we study in detail the Hubble diagram and the Hubble law, while regarding the "Early measurement" we present how the primordial perturbations are produced during inflation, how they propagate until recombination, and finally, how they influence the anisotropies in the cosmic microwave background radiation.

**Notation and conventions:**
We will use natural units ($c = \hbar = k_B = 1$) and the metric signature will be $(+---)$. Regarding the indices: Greek indices ($\mu, \nu, ...$) run from 0 to 3, Latin indices ($i, j, ...$) will stand for spatial coordinates and we will use Einstein summation convention.
Moreover, the subscript 0 indicates that the quantity is evaluated at the present time $t_0$ (es: $a_0 := a(t_0)$), the dot above a quantity indicates the derivative with respect to time $t$ (es: $\dot{a} := \mathrm{d}a/\mathrm{d}t$), and the prime symbol indicates the derivative with respect to the conformal time $\tau$ (es: $a' := \mathrm{d}a/\mathrm{d}\tau$).

# 2 The cosmological model

In this section we will summarize the main features of the current cosmological model (the $\Lambda$ cold dark matter model), which will be essential for the following chapters. This section follows ref. [3] (also refs. [4] and [5] can be useful).

## 2.1 Geometry and dynamics

The standard cosmological model is built on the cosmological principle (the modern Copernican principle), which states that the universe is isotropic and homogeneous at large scales. On the basis of this principle, and on the validity of Einstein general relativity, we can constrain the form of the 4-dimensional metric to one dependent on just a parameter $k$ (the curvature) and a function of time $a(t)$ (the scale factor):

$$\begin{aligned} \mathrm{d}s^2 &= \mathrm{d}t^2 - a^2(t)\left[\mathrm{d}\boldsymbol{x}^2 + k\frac{(\boldsymbol{x}\cdot\mathrm{d}\boldsymbol{x})^2}{1-k\boldsymbol{x}^2}\right] = \mathrm{d}t^2 - a^2(t)\left[\frac{\mathrm{d}r^2}{1-kr^2} + r^2\mathrm{d}\Omega^2\right] \\ &= \mathrm{d}t^2 - a^2(t)\left[\mathrm{d}\chi^2 + S_k^2(\chi)\mathrm{d}\Omega^2\right] \end{aligned} \tag{1}$$

where

$$S_k(\chi) := \begin{cases} \sinh\chi & \text{if } k=-1 \\ \chi & \text{if } k=0 \\ \sin\chi & \text{if } k=+1 \end{cases} = \chi + O\left(\chi^3\right) \qquad \text{and} \qquad \mathrm{d}\Omega^2 := \mathrm{d}\theta^2 + \sin^2\theta\mathrm{d}\phi^2 \tag{2}$$

This is called the Friedmann–Lemaître–Robertson–Walker (FLRW) line element. It is expressed in the standard Cartesian coordinates $\boldsymbol{x}$, in the spherical polar coordinates $(r,\theta,\phi)$ and in the spherical coordinates $(\chi,\theta,\phi)$ where $\mathrm{d}\chi := \frac{\mathrm{d}r}{\sqrt{1-kr^2}}$.
It is possible to fix the normalization of the scale factor (which, indeed, is not a physical quantity) so to have $k \in \{0,\pm1\}$ or $a_0 = 1$. The coordinates $\boldsymbol{x}$ are called comoving coordinates and the so called "proper" physical distance at a fixed time $t$ between a point at the orgin and one at radial coordinate $r$ is therefore:

$$\boldsymbol{d}_P := a(t)\int_0^r \frac{\mathrm{d}\tilde{r}}{\sqrt{1-k\tilde{r}^2}}\boldsymbol{u}_r = a\chi\boldsymbol{u}_r \tag{3}$$

Finally $\boldsymbol{d}_m := aS_k(\chi)\boldsymbol{u}_r$ is called metric distance. For two fixed comoving observer, one finds:

$$\boldsymbol{v}_P := \frac{d}{dt}\boldsymbol{d}_P = \frac{d}{dt}\left[a(t)\int_0^r \frac{\mathrm{d}\tilde{r}}{\sqrt{1-k\tilde{r}^2}}\right]\boldsymbol{u}_r = H(t)\boldsymbol{d}_P \tag{4}$$

where $H(t) := \dot{a}/a$ and $\boldsymbol{v}_P$ is the physical velocity. This expression evaluated at $t = t_0$ is called the Hubble law, and $H_0$ the Hubble constant.
It is possible to associate a redshift $z := \lambda_r/\lambda_e - 1$ to every light signal that we receive, constructed from the ratio between the received and the emitted wavelength. Using the FLRW metric and the general relativity formula for the gravitational redshift, we can demonstrate [3], respectively, (associating $\lambda_r$ to the wavelength $\lambda_0$ observed today) that: $1 + z = a_0/a$ and $z \sim |\boldsymbol{v}| \sim H_0 d_P$ (for nearby objects).
The convenience of using the variable $z$ is that, unlike $\boldsymbol{x}$ or $\boldsymbol{d}_P$, it is an observable (namely, a quantity that can be directly measured). We can relate it to two other observable quantities, introduced to quantify our spatial distance form a cosmological object:

- the luminosity distance, defined as $d_L := \sqrt{\frac{F}{4\pi L}}$ where L is the absolute luminosity (energy emitted per second) of a cosmic source and F is the observed flux (energy per second per receiving area) from the earth. It is possible to demonstrate [3] that $d_L = d_m(1+z)$;
- the angular distance, defined as $d_A := \frac{D}{\delta\theta}$ where D is the physical size of a cosmic object and $\delta\theta$ is the angular size measured from earth, and since $D = a(t_e)S_k(\chi)\delta\theta$ therefore $d_A = \frac{d_m}{1+z}$.

To determine the time evolution of these distances we can employ the Einstein equations:

$$G_{\mu\nu} = 8\pi G T_{\mu\nu} - \Lambda g_{\mu\nu} \tag{5}$$

where $\Lambda$ is the cosmological constant, $T_{\mu\nu}$ is the stress-energy-momentum (s.e.m.) tensor for all the fields present in the universe and $G_{\mu\nu}$ is the Einstein tensor that is built from the Levi Civita connection of the metric ${\Gamma^\lambda}_{\mu\nu}$ in the following way:

$$G_{\mu\nu} := R_{\mu\nu} - \frac{1}{2} g_{\mu\nu} R \,, \qquad R_{\mu\nu} := {R^\sigma}_{\mu\sigma\nu} \,, \qquad R := {R^\mu}_\mu$$

$${R^\lambda}_{\sigma\mu\nu} := \partial_\mu {\Gamma^\lambda}_{\sigma\nu} - \partial_\nu {\Gamma^\lambda}_{\sigma\mu} + {\Gamma^\lambda}_{\mu\rho}{\Gamma^\rho}_{\nu\sigma} - {\Gamma^\lambda}_{\nu\rho}{\Gamma^\rho}_{\mu\sigma} \,, \qquad {\Gamma^\lambda}_{\mu\nu} := \frac{1}{2} g^{\lambda\rho} \left(\partial_\mu g_{\nu\rho} + \partial_\nu g_{\mu\rho} - \partial_\rho g_{\mu\nu}\right) \tag{6}$$

where $g_{\mu\nu}$ is the metric of the universe and $g^{\mu\nu}$ is its inverse.
We evaluate the Einstein tensor for a FLRW geometry. We then choose the s.e.m. that approximates our universe best at the (large) scales in which the cosmological principle is valid, namely the s.e.m. tensor of a motionless perfect fluid i.e. ${T^\mu}_\nu = (\rho + P) U^\mu U_\nu - P {\delta^\mu}_\nu$ , with $U^\mu = (1,0,0,0)^T$ the 4−velocity, $\rho$ the energy density, and $P$ the pressure of a perfect fluid in its rest frame.
At this point we can derive the scale factor differential equations writing the nontrivial components of the Einstein equations, as well as a conservation law $\nabla_\mu {T^\mu}_\nu = \partial_\mu {T^\mu}_\nu + {\Gamma^\mu}_{\mu\lambda}{T^\lambda}_\nu - {\Gamma^\lambda}_{\mu\nu}{T^\mu}_\lambda = 0$ (that also follows from the Einstein equations):

$$\nabla_\mu {T^\mu}_0 = 0 \quad \Longrightarrow \quad \dot\rho + 3H(\rho + P) = 0 \qquad \text{(continuity equation)} \tag{7}$$

$${G^0}_0 = 8\pi G {T^0}_0 - \Lambda {g^0}_0 \quad \Longrightarrow \quad H^2 = \frac{8\pi G}{3}\rho - \frac{k}{a^2} + \frac{\Lambda}{3} \qquad \text{(I Friedmann equation)} \tag{8}$$

$${G^i}_i = 8\pi G {T^i}_i - \Lambda {g^i}_i \quad \forall i \quad \Longrightarrow \quad \frac{\ddot a}{a} = -\frac{4\pi G}{3}(\rho + 3P) + \frac{\Lambda}{3} \qquad \text{(II Friedmann equation)} \tag{9}$$

As already mentioned, these three equations are not independent, and one can for example obtiain the last one by differentiating the second equation 8 with respect to time, and then employing the first and second equation.
To solve these equations it is necessary to know the value of $\rho(t)$ and $P(t)$; neglecting interactions between the different species of matter (baryons, photons, neutrinos, ...), we can write $\rho(t)$ and $P(t)$ as the sum of all matter components contributes. As we will see better in the next subsection, it is possible to relate them into the equation of state $\rho = wP$, where $w$ is constant and takes the value $w = 0$ if the source is non-relativistic (dark matter, baryons, ...), $w = \frac{1}{3}$ if the source is relativistic (photons, neutrinos, gravitons, ...) and $w = -1$ if the source is vacuum energy. Thus if we use the equation of state into the continuity equation we can find the $a$ dependence of $\rho$ for each species at every time: $\rho \propto a^{-3(1+w)}$. From this it follows that for most of its history the universe was dominated by a single component, furthermore, comparing these dependencies with the observed values of the energy densities of the individual sources, we can find that the universe was dominated first by radiation, then matter and finally dark energy (see Figure 1). For each of these period the others non-dominant components can safely be ignored and hence, neglecting also the curvature (according to current estimates [7], $\Omega_k(t_0) := -k/(a_0^2 H_0^2) = 0.001 \pm 0.002$), we can integrate the first Friedmann equation and find that $a \propto t^{\frac{2}{3(1+w)}}$ for the radiation or matter domination period.
Finally, we need to include a source to account for the current stage of accelerated expansion. We can assume (see [7]) that this source is a vacuum energy (which acts as a cosmological constant) characterized by $w = -1$, and leading to $a \propto t^{Ht}$ (integrating the first Friedmann equation). Indeed, it is possible to describe the cosmological constant as if it were a fluid with energy density $\rho_\Lambda = \frac{\Lambda}{8\pi G}$ and pressure $P_\Lambda = -\rho_\Lambda$. In this way we can simplify the Friedmann equations replacing the cosmological constant with a new matter component that behaves like a dark energy component. Moreover if we define the critical density as the the density which would required in order to make the geometry of the universe flat at a time $t$ (i.e. $\rho_c(t) = \frac{3H^2}{8\pi G}$) hence it is possible to rewrite the first Friedmann equation in the following way:

$$1 = \Omega + \Omega_k = \left[\sum_i \Omega_i + \Omega_\Lambda\right] + \Omega_k \qquad \text{with} \;\; \Omega_{i/\Lambda}(t) = \frac{\rho_{i/\Lambda}}{\rho_c}, \;\; \Omega_k = -\frac{k}{a^2 H^2} \tag{10}$$

where the index $i$ runs through all the matter contents in the universe.

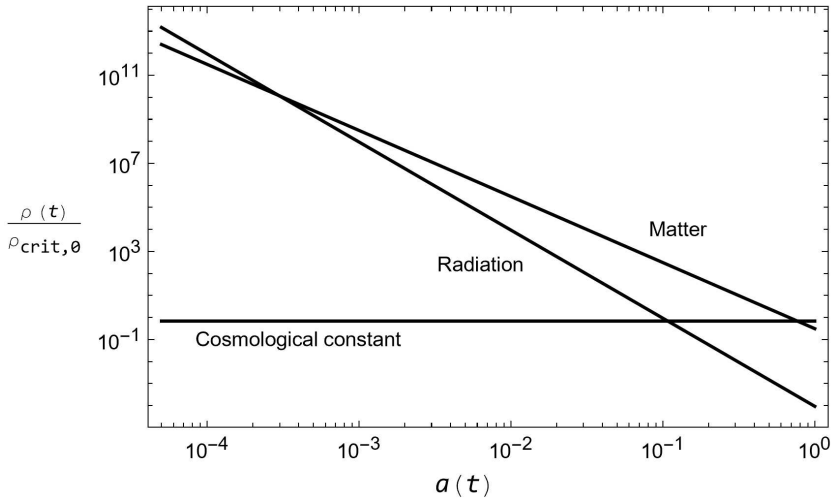


Figure 1: Evolution of energy densities in the universe. Data from ref. [7] and ref. [9].

## 2.2 Thermal history

The early universe was filled by different types of particles that interacted with each other as described by the Standard Model of partcle physics. When particles exchange energy and momentum efficiently, they reach thermal equilibrium end we can use the results of statistical mechanic to study the evolution of their number density $n$, energy density $\rho$ and pressure $P$. In particular, it is possible to establish if the interactions are efficient, and hence thermal equilibrium is reached by comparing the rates of these interactions $\Gamma := n\sigma v$ (where $v$ is the average velocity density of the particles and $\sigma$ is the interaction cross section, that we can estimate through the perturbative method of Feynman diagrams) with the expansion rate $H$. For $\Gamma > H$ the interactions are effective, while in the opposite regime the particles decouple from each other.
At early times the most of the particles were in thermal equilibrium with the others and so in that period the distribution $f(\boldsymbol{p})$ assumes the following form [3]:

$$n = \frac{g}{(2\pi)^3}\int \mathrm{d}^3p f(\boldsymbol{p}) \,, \qquad \rho = \frac{g}{(2\pi)^3}\int \mathrm{d}^3p f(\boldsymbol{p})E(\boldsymbol{p}) \,, \qquad P = \frac{g}{(2\pi)^3}\int \mathrm{d}^3p f(\boldsymbol{p})\frac{|\boldsymbol{p}|^2}{3E(\boldsymbol{p})}$$
$$\text{with} \quad f(\boldsymbol{p}) = \frac{1}{e^{(E(\boldsymbol{p})-\mu)/T} \pm 1} \,, \qquad E(\boldsymbol{p}) = \sqrt{m^2 + |\boldsymbol{p}|^2} \tag{11}$$

Where $g$ is the number of internal degrees of freedom of that species, $f(p)$ is the Fermi-Dirac (+1) and Bose-Einstein (-1) distribution and $\mu := -T(\frac{\partial S}{\partial N})_{U,V}$ is the chemical potential (which satisfies $\frac{\mu}{T} \ll 1$ ans so can be neglected in the present discussion).
In the relativistic limit, $T \gg m$, the three integrals give [3]:

$$n = \frac{\zeta(3)}{\pi^2} g T^3 \begin{cases} 1 & \text{for bosons} \\ \frac{3}{4} & \text{for fermions} \end{cases} \qquad \rho = \frac{\pi^2}{30} g T^4 \begin{cases} 1 & \text{for bosons} \\ \frac{7}{8} & \text{for fermions} \end{cases} \qquad P = \frac{1}{3}\rho \tag{12}$$

while in the non-relativistic limit, , $T \ll m$, they give:

$$n = g\left(\frac{mT}{2\pi}\right)^{3/2} e^{-m/T} \,, \qquad \rho \simeq mn \,, \qquad P \simeq nT \ll \rho \tag{13}$$

This justifies the equation of state $w = 1/3$ (respectively $w = 0$) for a relativistic (respectively, non relativistic) perfect fluid that we have employed in the previous section. More generally, it can be shown that the equations of state are satisfied even without assuming thermal equilibrium. Furthermore we can see that in the non-relativistic limit, when the temperature drops below the particle mass, the density is exponentially suppressed. We interpret this process as the annihilation of particles and anti-particles in the reaction $x + \bar{x} \to \gamma + \gamma$, which is no longer compensated by the opposite reaction.

We can now write the energy density of all the relativistic species as a function of their temperatures $T_i$ (we indicate with just $T$ the temperature of the photons and all the particles in thermal equilibrium with them):

$$\rho = \sum_i \rho_i = \frac{\pi^2}{30} g_\star(T) T^4 \,, \qquad \text{with} \quad g_\star(T) = \sum_{i=\text{bos}} g_i \left(\frac{T_i}{T}\right)^4 + \frac{7}{8} \sum_{i=\text{fer}} g_i \left(\frac{T_i}{T}\right)^4 \tag{14}$$

where we have introduced the effective number of relativistic degrees of freedom $g_\star(T)$. This result is useful also to find an approximated tread of the universe temperature decrease in function of time. Indeed using the I Friedmann equation and neglecting the subdominant non-relativistic component, we can find the following relation between temperature and time:

$$T \simeq 1.5 g_\star^{-1/4} \left(\frac{1 \text{ sec}}{t}\right)^{1/2} \quad \text{MeV} \tag{15}$$

Another important thermodynamic quantity is the entropy $S$ and its comoving density $s = S/V$. It is possible to show [3], through thermodynamic relations and the continuity equation, that $s = \frac{\rho + P}{T}$ and that $\frac{\mathrm{d}}{\mathrm{d}t} S = 0$, moreover for the previous considerations it follows that:

$$s = \sum_i \frac{\rho_i + P_i}{T_i} = \frac{2\pi^2}{45} g_{\star S}(T) T^3 \,, \qquad \text{with} \quad g_{\star S}(T) = \sum_{i=\text{bos}} g_i \left(\frac{T_i}{T}\right)^3 + \frac{7}{8} \sum_{i=\text{fer}} g_i \left(\frac{T_i}{T}\right)^3 \tag{16}$$

Here we have defined the effective number of degrees of freedom in entropy $g_{\star S}(T)$. In the figure below 2 it is possible to see the evolution of $g_\star(T)$ (solid line) and $g_{\star S}(T)$ (dotted line) in a numerical integration that assumes the Standard Model particle content. The figure also shows the temperatures at which a specific species annihilates and thus the effective number of degrees of freedom experience a rapid drop.

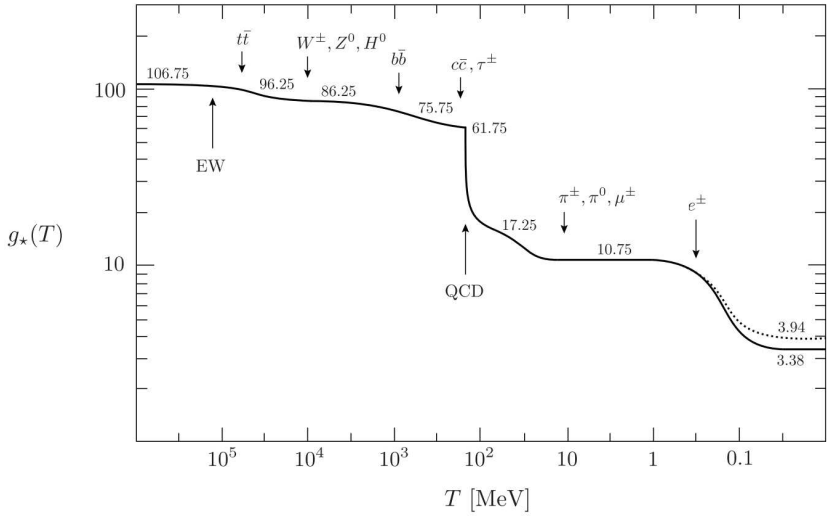


Figure 2: Evolution of relativistic degrees of freedom $g_\star(T)$ assuming the Standard Model particle content. Figure taken from ref. [3].

## 2.3 Cosmological perturbation theory

So far, we have treated the universe as perfectly homogeneous. To understand the formation and evolution of CMB and large scale structure (LSS), we have to introduce inhomogeneities ($\delta g_{\mu\nu}$, $\delta\rho$, $\delta P$, $\delta U^\mu$). This significantly complicates the computations since, unlike Maxwell equations, Einstein equations are nonlinear. We can however exploit the fact that inhomogeneities are small at large scales (as testified by the fact that the CMB temperature anisotropies are of the order of $\frac{\delta T}{T} \sim 10^{-5}$). This allows to set-up a pertrubative scheme in which Einstein equations are written and solved order by order in the perturbations. We discuss here only the linearized order, which is enough to explain the main characteristics of the CMB physics.

### 2.3.1 Perturbations of the metric

We use conformal time $\tau$, related to the physical time $t$ used in eq. 1 by $\mathrm{d}\tau = \mathrm{d}t/a(t)$, and we focus our attention to a flat FLRW geometry. The most general set of perturbations of this geometry reads:

$$g_{\mu\nu} = \bar{g}_{\mu\nu} + \delta g_{\mu\nu} \qquad ds^2 = a^2(\tau)\left[(1+2A)d\tau^2 - 2B_i dx^i d\tau - (\delta_{ij} + h_{ij})dx^i dx^j\right] \tag{17}$$

with $A$, $B_i$ and $h_{ij}$ functions of space and time, and $h_{ij} = h_{ji}$ since the metric must be symmetrical. It is extremely useful to perform a scalar-vector-tensor (SVT) decomposition of the perturbations. The SVT decomposition follows from Helmholtz theorem and makes possible to decompose the 10 degrees of freedom of linearized perturbations of the FRW metric (eq. 17) into components according to their transformations under spatial rotations, in particular: four scalar fields ($4 \cdot 1 = 4$ d.o.f.), two divergence-free spatial vector fields ($2 \cdot 2 = 4$ d.o.f.), and a traceless, symmetric and divergence-free spatial tensor field ($1 \cdot 2 = 2$ d.o.f.).
What justifies this complex procedure and makes the SVT decomposition so powerful is the fact that the Einstein equations for scalars, vectors and tensors do not mix at linear order and can therefore be treated separately. Therefore, the decomposition $(A,\ B_i,\ h_{ij}) \to (A,\ B,\ C,\ E,\ \hat{B}_i,\ \hat{E}_i,\ \hat{E}_{ij})$ will be:

$$B_i = \partial_i B + \hat{B}_i\ , \qquad h_{ij} = 2C\delta_{ij} + 2\partial_{\langle i}\partial_{j\rangle}E + \partial_{(i}\hat{E}_{j)} + 2\hat{E}_{ij} \tag{18}$$

$$\partial_{\langle i}\partial_{j\rangle}E := \left(\partial_i\partial_j - \frac{1}{3}\delta_{ij}\nabla^2\right)E\ , \qquad \partial_{(i}\hat{E}_{j)} := \frac{1}{2}\left(\partial_i\hat{E}_j + \partial_j\hat{E}_i\right) \tag{19}$$

with $\partial^i\hat{B}_i = \partial^i\hat{E}_i = \partial^i\hat{E}_{ij} = \hat{E}^i{}_i = 0$.
When we define these functions we have to choose a particular spacetime coordinates $(\tau, \boldsymbol{x})$ to parameterize them, making a different choice of coordinates (or gauge choice) $X^\mu \to \tilde{X}^\mu = \tilde{X}^\mu(X)$ can change the metric and so the values of the perturbation functions. Indeed the Einstein theory ensures invariance of the interval $\mathrm{d}s^2$ under any spacetime reparametrizations:

$$\mathrm{d}s^2 = g_{\mu\nu}(X)\mathrm{d}X^\mu\mathrm{d}X^\nu = \tilde{g}_{\alpha\beta}(\tilde{X})\mathrm{d}\tilde{X}^\alpha\mathrm{d}\tilde{X}^\beta, \qquad g_{\mu\nu}(X) = \frac{\partial\tilde{X}^\alpha}{\partial X^\mu}\frac{\partial\tilde{X}^\beta}{\partial X^\nu}\tilde{g}_{\alpha\beta}(\tilde{X}) \tag{20}$$

Once we apply this reparametrization to the perturbed geometry (eq. 17), we deduce that not all the 10 perturbation parameters are physically independent quantities. In order to remove the ambiguity and to make easier the treatment it is necessary to choose and fix a gauge choice.
Since we are interested in a first order expansion we can consider an infinitesimal coordinates transformation $X^\mu \to \tilde{X}^\mu = X^\mu + \xi^\mu(\tau, \boldsymbol{x})$ and the relative SVT decomposition $\xi^0 = T,\ \ \xi^i = L_i = \partial_i L + \hat{L}_i$. Using this transformation in equation 20 we can find how the parameters of perturbed metric transform [3]:

$$A \to \tilde{A} = A - T' - \mathcal{H}T\ , \qquad B_i \to \tilde{B}_i = B_i + \partial_i T - L_i'\ , \qquad h_{ij} \to \tilde{h}_{ij} = h_{ij} - 2\partial_{(i}L_{j)} - 2\mathcal{H}T\delta_{ij} \tag{21}$$

where $\mathcal{H} := a'/a = aH$. And in terms of the SVT decomposition we get:

$$A \to A - T' - \mathcal{H}T\ , \qquad B \to B + T - L'\ , \qquad \hat{B}_i \to \hat{B}_i - \hat{L}_i' \tag{22}$$

$$C \to C - \mathcal{H}T - \frac{1}{3}\nabla^2 L\ , \qquad E \to E - L\ , \qquad \hat{E}_i \to \hat{B}_i - \hat{L}_i\ , \qquad \hat{E}_{ij} \to \hat{E}_{ij} \tag{23}$$

where $\mathcal{H} := a'/a$ is the Hubble parameter in conformal time. It is possible to define special combinations of metric perturbations that do not transform under a change of coordinates. These are the Bardeen variables [12]:

$$\Psi := A + \mathcal{H}(B - E') + (B - E')\ , \qquad \Phi := -C - \mathcal{H}(B - E') + \frac{1}{3}\nabla^2 E\ , \qquad \hat{\Psi}_i := \hat{E}_i' - \hat{B}_i\ , \qquad \hat{E}_{ij} \tag{24}$$

Concerning the scalar perturbations, we can use the freedom in the gauge functions T and L to set two of the four scalar metric perturbations to zero (this is called gauge fixing). The choice to set $B = E = 0$ is called the Newtonian gauge and it gives the metric:

$$\mathrm{d}s^2 = a^2(\tau)\left[(1+2\Psi)\mathrm{d}\tau^2 - (1-2\Phi)\delta_{ij}\mathrm{d}x^i\mathrm{d}x^j\right] \qquad \text{with} \quad \Psi = A,\ \Phi = -C \tag{25}$$

where we have ignored the non-scalar perturbations. Furthermore, as we will see better later, $\Psi$ plays the role of the gravitational potential and the absence of anisotropic stress implies $\Psi = \Phi$.
In this dissertation we will use only the Newtonian gauge.

### 2.3.2 Perturbations of the stress-energy-momentum tensor

Analogously to what we did for the geometry ($\delta g_{\mu\nu}$), we now perturb the s.e.m. tensor ($\delta T_{\mu\nu}$). We strart from the s.e.m. tensor for a single species, introducing $\delta\rho$, $\delta P$, $\delta U^\mu$ (functions of space and time) i.e. the perturbations of the homogeneous universe parameters $\bar\rho$, $\bar P$, $\bar U^\mu$ (functions of time). In this way the s.e.m. tensor at first order of perturbation becomes:

$$\delta T_{\mu\nu} = (\delta\rho + \delta P)\bar U_\mu \bar U_\nu + (\bar\rho + \bar P)(\delta U_\mu \bar U_\nu + \bar U_\mu \delta U_\nu) - \delta P \delta_{\mu\nu} - \Pi_{\mu\nu} \tag{26}$$

with $\Pi_{\mu\nu} = \Pi_{\nu\mu}$ and $\Pi^0{}_0 = \Pi^0{}_i = \Pi^i{}_i = 0$ (the 00 entry, the $0i$ entries an the spatial trace can always be absorbed into a redefinition of $\delta\rho$, $\delta U_i$, $\delta P$ respectively).
The 4-velocity $U^\mu = \bar U^\mu + \delta U^\mu$ has norm $+1$, namely, $U^\mu U_\mu = +1$. At the background level this implies $\bar U^\mu = a^{-1}\delta^\mu_0$. At the perturbative level, this gives rise to:

$$g_{\mu\nu}U^\mu U^\nu = 1 \quad \xRightarrow{\text{1st order}} \quad \delta g_{\mu\nu}\bar U^\mu \bar U^\nu + 2\bar U^\mu \delta U_\mu = 0 \quad \Longrightarrow \quad \delta U^0 = -Aa^{-1} \tag{27}$$

Defining $\delta U^i := a^{-1}v^i$, we obtain $U^\mu = a^{-1}(1 - A, v^i)^T$. Using this result in equation 26 we finally find:

$$\delta T^0{}_0 = \delta\rho\,, \qquad \delta T^i{}_0 = q^i\,, \qquad \delta T^0{}_i = -[q_i + (\bar\rho + \bar P)B_i]\,, \qquad \delta T^i{}_j = -\delta P \delta^i_j - \Pi^i{}_j \tag{28}$$

where we have defined $q^i := (\bar\rho + \bar P)v^i$, the momentum density.

The total s.e.m. tensor is obtained by summing the contributions of all species (photons, baryons, dark matter, ...), $T_{\mu\nu} = \sum_I T^I_{\mu\nu}$. This gives:

$$\delta\rho = \sum_I \delta\rho_I\,, \qquad \delta P = \sum_I \delta P_I\,, \qquad q^i = \sum_I q^i_I\,, \qquad \Pi^{ij} = \sum_I \Pi^{ij}_I \tag{29}$$

The velocities do not add, but the momentum densities do. At this point it is possible to proceed as done with the metric perturbations.
Applying the SVT decomposition to the perturbations:

$$\delta\rho\,, \qquad \delta P\,, \qquad v_i = \partial_i v + \hat v_i\,, \qquad q_i = \partial_i q + \hat q_i\,, \qquad \Pi_{ij} = \partial_{\langle i}\partial_{j\rangle}\Pi + \partial_{(i}\hat\Pi_{j)} + \hat\Pi_{ij} \tag{30}$$

Evaluating how perturbations transform under the infinitesimal coordinate transformation $\xi^0 = T$, $\xi^i = L_i = \partial_i L + \widehat{L}_i$:

$$\delta\rho \to \delta\rho - T\bar\rho'\,, \qquad \delta P \to \delta P - T\bar P'\,, \qquad v_i \to v_i + L_i'\,, \qquad q_i \to q_i + (\bar\rho + \bar P)L_i'\,, \qquad \Pi_{ij} \to \Pi_{ij} \tag{31}$$

And finally defining gauge invariant quantities, as the comoving gauge density:

$$\Delta := \frac{\delta\rho + \bar\rho'(v + B)}{\bar\rho} \quad \xrightarrow{\text{Newtonian gauge}} \quad \Delta = \frac{\delta\rho + \bar\rho' v}{\bar\rho} \tag{32}$$

Above we used our gauge freedom to set two of the scalar metric perturbations to zero (Newtonian gauge). Alternatively we could use the gauge fixing in the matter sector, for example setting $\delta\rho = 0$ (uniform density gauge) or $q = 0$ (comoving gauge).

### 2.3.3 Linearized evolution equations

Having found the expression for $\delta g_{\mu\nu}$ and $\delta T_{\mu\nu}$, we can obtain the perturbed Einstein equation $\delta G_{\mu\nu} = 8\pi G\, \delta T_{\mu\nu}$ through the linearization of equations 6. Since, in this dissertation, we are interested only in scalar fluctuations (first-order vector perturbations are not generated during inflation and tensor modes are negligible), we consider only their contribution in the expression of $\delta g_{\mu\nu}$ and $\delta T_{\mu\nu}$, therefore we will find Einstein Equation as a function of $\Psi$, $\Phi$, $\delta\rho$, $\delta P$, $v$, $\Pi$. As we did in the first subsection we start by computing the continuity equation:

$$\nabla_\mu\, \delta T^\mu{}_0 = 0 \quad \Longrightarrow \quad \delta' + 3\mathcal{H}\left(\frac{\delta P}{\delta\rho} - \frac{\bar{P}}{\bar{\rho}}\right)\delta = -\left(1 + \frac{\bar{P}}{\bar{\rho}}\right)(\boldsymbol{\nabla}\cdot\boldsymbol{v} - 3\Phi') \tag{33}$$

$$\nabla_\mu\, \delta T^\mu{}_i = 0 \;\; \forall i \quad \Longrightarrow \quad \boldsymbol{v}' + 3\mathcal{H}\left(\frac{1}{3} - \frac{\bar{P}}{\bar{\rho}}\right)\boldsymbol{v} = -\frac{\boldsymbol{\nabla}\delta P}{\bar{\rho} + \bar{P}} - \boldsymbol{\nabla}\Psi \tag{34}$$

where $\delta := \delta\rho/\bar{\rho}$ and $\boldsymbol{v} = \boldsymbol{\nabla} v$.
These two expressions are the linearized general relativity generalization of, respectively, the continuity $\partial_t \rho = \boldsymbol{\nabla}\cdot(\rho\boldsymbol{v})$ and Navier–Stokes equations $(\boldsymbol{v}\cdot\boldsymbol{\nabla})\cdot\boldsymbol{v} = -\frac{1}{\rho}\boldsymbol{\nabla}P + \nu\nabla^2\boldsymbol{v} - \boldsymbol{\nabla}\Phi$.

$$\delta G_{ij} = 8\pi G\, \delta T_{ij} \quad i \neq j \quad \Longrightarrow \quad \partial_{\langle i}\partial_{j\rangle}(\Psi - \Phi) = 8\pi G a^2\, \partial_{\langle i}\partial_{j\rangle}\Pi \tag{35}$$

The anisotropic stress $\Pi_{ij}$ is negligible in the early universe, and we can disregard it [3]. Therefore $\Pi = 0 \implies \partial_{\langle i}\partial_{j\rangle}(\Psi - \Phi) = 0 \implies \Psi = \Phi$ . In the absence of anisotropic stress there is then only one gauge-invariant degree of freedom in the metric. In the following we will write all equations in terms of $\Phi$.

$$\delta G_{00} = 8\pi G\, \delta T_{00} \quad \Longrightarrow \quad \nabla^2\Phi - 3\mathcal{H}(\Phi' + \mathcal{H}\Phi) = 4\pi G a^2 \delta\rho \tag{36}$$

$$\delta G_{0i} = 8\pi G\, \delta T_{0i} \;\; \forall i \quad \Longrightarrow \quad \Phi' + \mathcal{H}\Phi = -4\pi G a^2(\bar{\rho} + \bar{P})v \tag{37}$$

$$\text{eq. 36} \;+\; \text{eq. 37} \quad \Longrightarrow \quad \nabla^2\Phi = 4\pi G a^2 \bar{\rho}\Delta \tag{38}$$

$$\delta G_{ii} = 8\pi G\, \delta T_{ii} \;\; \forall i \quad \Longrightarrow \quad \Phi'' + 3\mathcal{H}\Phi' + (2\mathcal{H}' + \mathcal{H}^2)\Phi = 4\pi G a^2 \delta P \tag{39}$$

We can notice that equation 38 represents the linearized generalization of Poisson equation $\nabla^2\Phi = 4\pi G\rho$ of Newtonian gravity.
Finally it is important to notice that this set of equations is consistent but redundant. Indeed Einstein equations imply continuity equations (Bianchi identity) and, obviously, equation 36 plus equation 37 imply equation 38.

### 2.3.4 Initial conditions from inflation

Einstein equations (zeroth and first order) govern the evolution of the background physical quantities and their perturbations during the universe evolution. However, to compute these quantities, we need to know their initial conditions. By initial condition here we mean their values at the end of inflation, and at the beginning of he standard "hot big-bang era". We denote this time as $t_{\rm in}$. Concerning the background quantities (studied in the first subsection), we used the value of parameters (like $\Omega_{\rm mat}$, $\Omega_{\rm rad}$, $H$...) evaluated at present time $t = t_0$, and rescaled back to $t_{\rm in}$. To study the evolution of perturbations, instead, we have to use the value of them right after inflation at $t = t_{\rm in}$. In this dissertation we discuss how inflation provides the initial conditions for the perturbations in the following era. The simplest predictions of inflation are [3]:

- the perturbations follow a Gaussian statistics;
- primordial perturbations are almost scale-independent;
- the initial matter fluctuations were adiabatic fluctuations (namely there is only one independent scalar degree of freedom);
- for adiabatic perturbations all the predictions for the metric and s.e.m tensor perturbations can be given in terms of a single curvature perturbation $\zeta(t_{\rm in}, \boldsymbol{x})$.

Regarding the first two statements, they will be useful dealing with the CMB measures in the next section, and so in that chapter we will go into detail.
Concerning adiabatic fluctuation, they are a particular type of matter perturbations where the local state of matter $(\rho, P, v, ...)$ at some spacetime point $(\tau,\ \boldsymbol{x})$ of the perturbed universe is the same as in the background universe at some slightly different time $\tau + \delta\tau(\boldsymbol{x})$, where $\delta\tau$ is the same for all species. Namely, using the density perturbation of a species $I$ as an example:

$$\delta\rho_I(\tau, \boldsymbol{x}) := \bar{\rho}_I(\tau + \delta\tau(\boldsymbol{x})) - \bar{\rho}_I(\tau) \approx \dot{\bar{\rho}}_I \delta\tau(\boldsymbol{x}) \tag{40}$$

Since $\delta\tau(\boldsymbol{x})$ is the same for all species $I$, using continuity equation and the equation of state:

$$\delta\tau = \frac{\delta\rho_I}{\bar{\rho}_I'} = \frac{\delta\rho_J}{\bar{\rho}_J'} \quad \Longrightarrow \quad \frac{\delta_I}{1+w_I} = \frac{\delta_J}{1+w_J} \qquad \text{(for all species } I \text{ and } J) \tag{41}$$

with $\delta_{I,J} := \delta\rho_{I,J}/\bar{\rho}_{I,J}$ the fractional density contrast.
We notice that all matter perturbations at $\tau = 0$ can be characterized by a single degree of freedom $\delta\tau(\boldsymbol{x})$ and that the total density perturbation is dominated by the species that is dominant in the background since all the $\delta_I$ are comparable.
The complement of adiabatic perturbations are isocurvature perturbations, characterized by:

$$S_{IJ} := \frac{\delta_I}{1+w_I} - \frac{\delta_J}{1+w_J} \tag{42}$$

which can be sourced in multi-field inflation (which is a possibility that we do not consider in this dissertation).
Concerning the curvature perturbation that we have chosen to employ (we could represent the initial conditions in another way), it is a scalar field defined as:

$$\psi := C - \frac{1}{3}\nabla^2 E \tag{43}$$

It can be related to the three-dimensional Ricci scalar $R_{(3)}$, associated with the spacial part of the perturbed metric (eq. 17) $-a^2(\delta_{ij} + h_{ij})$: $a^2 R_{(3)} = -4\nabla^2\psi$ (for the proof see [3]).
The mode $\psi$ is not a gauge-invariant quantity, anyway it represents the value of two gauge-invariant expressions (see eq. 22, 23, 30) when computed in the comoving gauge ($B = q = 0$), or in the uniform density gauge ($\delta\rho = 0$). Specifically:

- comoving curvature perturbation: $\mathcal{R} := C - \frac{1}{3}\nabla^2 E + \mathcal{H}(B + v)$
- uniform energy density curvature perturbation: $\zeta := C - \frac{1}{3}\nabla^2 E - \mathcal{H}\frac{\delta\rho}{\bar{\rho}'}$

Working whit $\mathcal{R}$ in Newtonian gauge we obtain:

$$\mathcal{R} = -\Phi + \mathcal{H}v \quad \Longrightarrow \quad \mathcal{R} = -\Phi - \frac{\mathcal{H}(\Phi' + \mathcal{H}\Phi)}{4\pi G a^2(\bar{\rho} + \bar{P})} \tag{44}$$

where we have used equation 37 in order to eliminate the peculiar velocity in favour of the gravitational potential and its time derivative. Moreover, if a single component dominates the universe and the perturbations are adiabatic, we can use the first Friedmann equation and the equation of state to find:

$$\mathcal{R} = -\Phi - \frac{2}{3(1+w)}\left(\frac{\Phi'}{\mathcal{H}} + \Phi\right) \tag{45}$$

We want to prove that the curvature perturbation is conserved on large scales and for adiabatic perturbations. Therefore differentiating eq. 44 with respect to $\tau$ we obtain:

$$-4\pi G a^2(\bar{\rho} + \bar{P})\mathcal{R}' = 4\pi G a^2 \mathcal{H}\delta P_{\text{nad}} + \mathcal{H}\frac{\bar{P}'}{\bar{\rho}'}\nabla^2\Phi \qquad \text{with} \quad \delta P_{\text{nad}} := \delta P - \frac{\bar{P}'}{\bar{\rho}'}\delta\rho \tag{46}$$

where non-adiabatic pressure $\delta P_{\rm nad}$ vanishes for adiabatic fluctuations in a mixture of fluids that obey the equation of state $\rho = wP$. Therefore:

$$-4\pi G a^2(\bar{\rho}+\bar{P})\mathcal{R}' = \mathcal{H}\frac{\bar{P}'}{\bar{\rho}'}\nabla^2\Phi \quad \Longrightarrow \quad -4\pi G a^2(\bar{\rho}+\bar{P})\mathcal{R}' = -\mathcal{H}\frac{\bar{P}'}{\bar{\rho}'}k^2\Phi \tag{47}$$

$$\Phi(\boldsymbol{x},\tau),\ \mathcal{R}(\boldsymbol{x},\tau),\ \ldots \quad \longrightarrow \quad \Phi(\boldsymbol{k},\tau),\ \mathcal{R}(\boldsymbol{k},\tau),\ \ldots \tag{48}$$

where the arrows right hand side is the Fourier representation of the differential equation, performed via:

$$\Phi(\boldsymbol{x},\tau) = \frac{1}{(2\pi)^3}\int_{\mathbb{R}^3} \mathrm{d}^3k\ \ \Phi(\boldsymbol{k},\tau)\, e^{i\boldsymbol{k}\cdot\boldsymbol{x}} \tag{49}$$

This representation corresponds to identify a scalar field (in this case $\Phi(\boldsymbol{x},\tau)$) as a continuous sum (integral) of plane wave solution, each one caracterized by the constant comoving wavevector $\boldsymbol{k}$, called modes. Each mode is "weighted" by a suitable coefficient (in this case $\Phi(\boldsymbol{k},\tau)$) that expresses its magnitude and phase. We often employ this representation in the following sections.
If we now consider $\mathcal{R}(\boldsymbol{k},\tau)$ and $\Phi(\boldsymbol{k},\tau)$ related to modes with small $k = |\boldsymbol{k}|$ ($k \ll \mathcal{H}$, superhorizon modes), we can obtain that $\mathcal{R} \sim \Phi$ (we will prove it in the next subsection) and therefore, using eq. 47, that:

$$\mathcal{H}^2\mathcal{R}' \sim \mathcal{H}k^2\mathcal{R} \quad \Longrightarrow \quad \frac{\mathrm{d}\ln\mathcal{R}}{\mathrm{d}\ln a} \sim \left(\frac{k}{\mathcal{H}}\right)^2 \sim 0 \qquad \text{(superhorizion)} \tag{50}$$

Therefore, since $k$ represent the inverse of the characteristic comoving length of the mode ($k = 1/\lambda$) and $\mathcal{H}$ represent the inverse of the characteristic conformal time of the universe expansion ($\mathcal{H} = 1/\tilde{\tau}$), this equation is the formalization of the concept that large-scale perturbations are not modified until the different regions of the mode becomes casually connected ($k \sim \mathcal{H} \implies \lambda \sim c\tilde{\tau}$, horizon crossing). To resume, any mode of interest for observations today was outside the Hubble radius if we go back sufficiently far into the past. Inflation sets the initial condition for these superhorizon modes through the curvature perturbation, which is frozen until it re-enters inside the horizon.
Finally, it is possible to demonstrate (see [17]) that $\zeta$ and $\mathcal{R}$ are equal at superhorizon scales (to first order in the perturbations). Specifically:

$$\zeta = \mathcal{R} - \frac{2}{9(1+w)}\left(\frac{k}{\mathcal{H}}\right)^2\Psi \quad \Longrightarrow \quad \zeta \sim \mathcal{R} \qquad \text{(superhorizion)} \tag{51}$$

Therefore, the initial perturbative conditions generated by inflation, which are well described in terms of $\zeta$, coincide with those of $\mathcal{R}$ since all modes were outside the horizon at the end of inflation. Hence, also $\zeta$ is constant at superhorizon scales (for adiabatic perturbations).

### 2.3.5 Evolution of gravitational potential

In this last subsection we want to derive the behavior of the gravitational potential from $\tau = \tau_{\rm in}$ to recombination, this behavior is governed by Einstein equations. Through eq. 36, eq. 39 and the two Friedmann equations, converted to conformal time $\tau$ (using $H = \mathcal{H}/a$ and $\dot{H} = \mathcal{H}'/a^2 - \mathcal{H}^2/a^2$), we can find a closed form evolution equation for the gravitational potential:

$$\Phi'' + 3(1+w)\mathcal{H}\Phi' - w\nabla^2\Phi = 0 \quad \Longrightarrow \quad \Phi'' + 3(1+w)\mathcal{H}\Phi' + wk^2\Phi = 0 \tag{52}$$

where the arrow right hand side is the Fourier representation.
Concerning, instead, initial condition of this differential equation $\Phi(\boldsymbol{x},\tau_{\rm in})$, they can be derived from the initial conditions of the curvature perturbation parameter that, as we have said before, it is the most convenient way to represent the evolution of inflation perturbations at time $\tau = \tau_{\rm in}$. Since we are studying $\Phi$ and $\mathcal{R}$ at time $\tau = \tau_{\rm in}$ we can assume that all modes are superhorizon ($k \ll \mathcal{H}$). In this situation equation 52 imply $\Phi' = 0 \implies \Phi(\tau) = const.$. Moreover, this and eq. 45 imply:

$$\mathcal{R} = -\frac{5+3w}{3+3w}\Phi \quad \Longrightarrow \quad \mathcal{R} = -\frac{3}{2}\Phi_{\rm RD} = -\frac{5}{3}\Phi_{\rm MD} \qquad \text{(superhorizion)} \tag{53}$$

Since at $\tau = \tau_{\rm in}$ the universe was radiation dominated, so $\Phi(\tau_{\rm in}) = -\frac{2}{3}\mathcal{R}(\tau_{\rm in})$. Therefore, in addition to the initial conditions, this implies that superhorizon modes of gravitational potential are constant all the time except during radiation-matter transition where they decrease by a factor of 9/10. Concerning subhorizon modes ($k \gtrsim \mathcal{H}$), we have to solve eq. 52 for radiation domination and matter domination era separately:

- In the radiation era, $w = 1/3$, we get:

$$\Phi_{\boldsymbol{k}}'' + \frac{4}{\tau}\Phi_{\boldsymbol{k}}' + \frac{k^2}{3}\Phi_{\boldsymbol{k}} = 0 \quad \Longrightarrow \quad \Phi_{\boldsymbol{k}}(\tau) = A_{\boldsymbol{k}}\frac{j_1(x)}{x} + B_{\boldsymbol{k}}\frac{n_1(x)}{x}, \qquad x := \frac{k\tau}{\sqrt{3}} \tag{54}$$

  where the functions $j_1(x)$ and $n_1(x)$ are the spherical Bessel and Neumann functions:

$$j_1(x) := \frac{\sin x}{x^2} - \frac{\cos x}{x} = \frac{x}{3} + O\left(x^3\right) , \qquad n_1(x) := -\frac{\cos x}{x^2} - \frac{\sin x}{x} = -\frac{1}{x^2} + O\left(1\right) \tag{55}$$

  By setting the initial conditions ($B_{\boldsymbol{k}} = 0$ since $n_1 \to -\infty$ for $x \to 0$, and $\Phi_{\boldsymbol{k}}(\tau_{\rm in}) = -\frac{2}{3}\mathcal{R}_{\boldsymbol{k}}(\tau_{\rm in})$ as we have seen before) we find that:

$$\Phi_{\boldsymbol{k}}(\tau) = -2\mathcal{R}_{\boldsymbol{k}}(\tau_{\rm in})\left(\frac{\sin(x - x_{\rm hc}) - (x - x_{\rm hc})\cos(x - x_{\rm hc})}{(x - x_{\rm hc})^3}\right) \qquad \text{(all scales, } w = 1/3\text{)} \tag{56}$$

  with $x_{\rm hc} := (k\tau_{\rm hc})/\sqrt{3}$ and $\tau_{\rm hc}$ the conformal time at the horizon crossing of the perturbation $k = \mathcal{H}(\tau_{\rm hc})$.

- In the matter era, w = 0, instead the evolution of the potential is:

$$\Phi'' + \frac{6}{\tau}\Phi' = 0 \quad \Longrightarrow \quad \Phi \propto \begin{cases} const. \\ \tau^{-5} \propto a^{-5/2} \end{cases} \quad \Longrightarrow \quad \Phi = const. \qquad \text{(all scales, } w = 0\text{)} \tag{57}$$

  where we have disregarded the decaying mode $\Phi \propto \tau^{-5}$.

Figure 3 shows the evolution of the gravitational potential, from a numerical simulation, for three mode of different wavelength $\lambda = k^{-1}$. As predicted, the potential is constant while the modes are

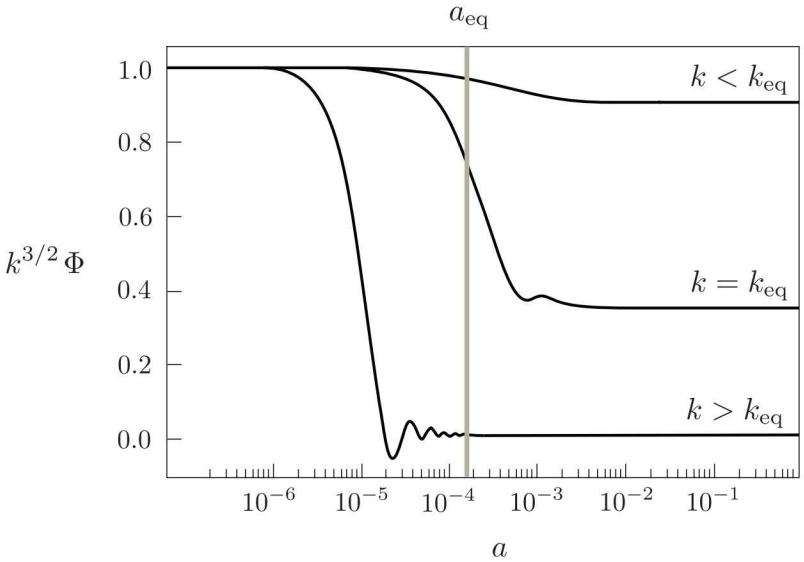


Figure 3: Numerical solutions for the linear evolution of the gravitational potential. We recall that $k_{\rm eq} = \mathcal{H}(t_{\rm eq})$, where "eq" refers to the radiation-matter transition. From top to bottom, the modes shown re-enter the horizon, respectively, during the matter-dominated era, at radiation-matter equality, and during the radiation-dominated era. Figure taken from ref. [3].

outside the horizon. The mode shown with $k < k_{\rm eq}$ enter the horizon during the matter era, and therefore its amplitude is constant all the time ecxept for the suppression of a 9/10 factor during the

radiation-matter transition. The two other modes shown re-enter the horizon at the radiation-matter equality or during the radiation era. Their amplitude decrease as $\tau^{-2} \sim a^{-2}$ during the radiation era, while their size is smaller or comparable to that of the horizon. The resulting amplitudes of these modes at the start of the matter era are therefore strongly suppressed as compared to that of the larger scale modes, that re-enter the horizon during the matter era. During the matter era the potential is constant on all scales.

# 3 The Hubble tension

The previous chapter describes the basis of the $\Lambda$ cold dark matter ($\Lambda$CDM) model. Nowadays, and in the past 30 years, it was the most important and widespread model and for this reason it is often called standard cosmological model. It is the simplest one that provides a good agreement with the datasets we have (including also Planck measurements). It makes several assumptions (all of them verified by measurements) and depends on only 6 fixed parameters. All the other physical quantities can be calculated from these. Some important assumptions of the model are: the presence of the cosmological constant (dark energy with $w = -1$) that drives the current accelerated expansion, the presence of non-relativistic (cold) dark matter that explains the large scale structure (LSS) we observe, the presence of a flat universe $k = 0$ (the current estimate is $\Omega_k = 0.001 \pm 0.002$, [7]).
While we have already considered the first two statements in the previous chapter, the last one can be used to simplify some equations we have derived. Indeed, since the universe is flat and it is possible to neglect the radiation density shortly some time after radiation matter equality, the Friedmann equation 8 is simplified and we can find an analytic solution of the scale factor for the relatively late universe composed of matter and dark energy:

$$a(t) = a_0 \left[\frac{(1-\Omega_\Lambda)}{\Omega_\Lambda}\right]^{1/3} \cdot \left[\sinh\left(\frac{3}{2}\sqrt{\Omega_\Lambda} H_0 t\right)\right]^{\frac{2}{3}}, \qquad t \gg t_{\text{RM equality}} \sim 60\,\text{kyr} \tag{58}$$

where the time axis origin is set at the singularity $a(0) = 0$ (where the solution is acually invalid).
As we have seen in the introduction, the $\Lambda$CDM model is currently under intense investigation [1], and the $\sim 5\sigma$ Hubble tension is one of the problems (see Figure 4). Indeed we have two main measurements of the Hubble constant $H_0$ that are in $\sim 5\sigma$ mutual disagreement. The one obtained from the CMB (including the most recent one by Placnk [7]) is called the "early measurement". On the contrary, the one inferred from physical events (such as supernovae) through distance and redshift measures in the local universe (including that provided by SH0ES Collaboration [8]) is called "late measurement". Both of the two measurements that characterize the Hubble tension are based on the same $\Lambda$CDM model, but they are influenced by its behavior in different epochs.
Armed with the concepts and results outlined in the previous sections, in the following sections we will briefly discuss the basic theoretical aspects of both measurements.

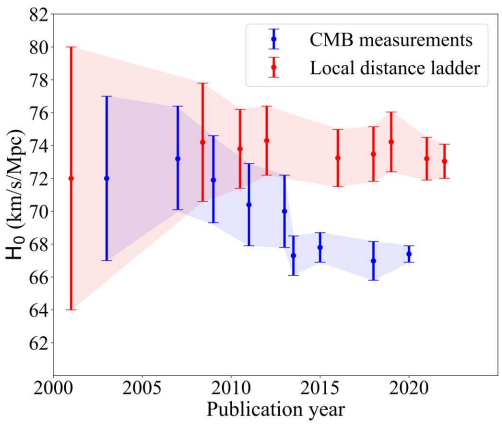


Figure 4: Some $H_0$ measurements form the 2000s to now. Figure taken from ref. [13].

### 3.1 Late measurement

The best established and most direct method to measure $H_0$ locally comes from measuring the distance-redshift relation of nearby celestial bodies ($z < 1$). Indeed, as we show in eq. 62, $H_0$ represent the first order relation between the luminosity distance and the redshift (both defined in the first section). In particular, the measures of distance are obtained by building a "distance ladder" (characterized by several methods used to estimate the distance of object at different scales of distance, each rung of the ladder provides information that can be used to determine the distances at the next higher rung). In 2005 the SH0ES (Supernovae, $H_0$, for the Equation of State of dark energy) project is started, this collaboration implements this method in order to estimate $H_0$. The last estimate, in agreement with the previous ones, is $H_0 = 73.2 \pm 1.3 \frac{\text{km}}{\text{sec Mpc}}$ [8].
In order to estimate the Hubble constant from the distance-redshift relation it is necessary to generalize the Hubble law (eq. 4) such that it relates two observable quantities, namely the luminosity distance and the redshift, that we can infer by measuring the radiation that comes from celestial bodies.
In the context of the ΛCDM model ($\Omega_k = 0$), using the definition of luminosity distance and the substitution $a \to z$ $\left(1 + z = \frac{a_0}{a(t)} \implies \mathrm{d}t = -\frac{a^2}{a_0 \dot{a}} \mathrm{d}z\right)$ we can find the analytic dependence of the distance on the redshift:

$$d_L(z) = a_0(1+z)\chi = a_0(1+z)\int_{t_e(z)}^{t_0} \frac{dt}{a(t)} = (1+z)\int_0^z \frac{d\tilde{z}}{H(\tilde{z})} \tag{59}$$

where $H(z) = H_0\sqrt{\Omega_r(1+z)^4 + \Omega_m(1+z)^3 + \Omega_\Lambda}$ (from the Friedmann equations).
Neglecting the radiation component (an excellent approximation well after the matter radiation equality, namely for these local measurements) we can also compute the integral:

$$d_L(z) = \frac{(1+z)\sqrt{1+R}}{H_0}\left[(1+z)H_{geom}\left(-R(1+z)^3\right) - H_{geom}(-R)\right] \tag{60}$$

with $R := \dfrac{1-\Omega_\Lambda}{\Omega_\Lambda}$ , and $H_{geom}(x) := {}_2F_1(\frac{1}{3}, \frac{1}{2}, \frac{4}{3}; x)$ is the hypergeometric function:

$${}_2F_1(a,b,c;z) := \sum_{n=0}^{\infty} \frac{(a)_n (b)_n}{(c)_n} \frac{z^n}{n!} \quad , \qquad (a)_n := \begin{cases} 1 & \text{if } n = 0 \\ a(a+1)(a+2)\cdots(a+n-1) & \text{if } n > 0 \end{cases}$$

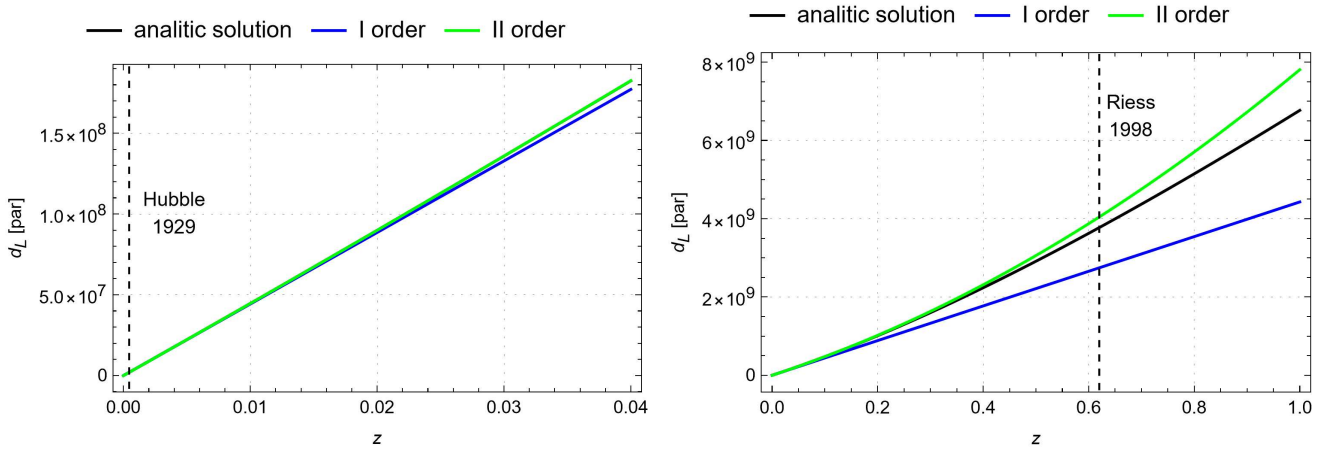


Figure 5: Luminosity distance (eq. 59) and its I and II order approximations (eq. 62), data from [7] and [9]. The vertical lines represent the maximum distance reached by E. Hubble in the discovery of the universe expansion [6] and by A.G Riess in the discovery of the acceleration of this expansion [10].

The first two derivatives of the luminosity distance with respect to the redshift read:

$$\frac{\partial d_L(z)}{\partial z} = \frac{d_L(z)}{1+z} + \frac{1+z}{H(z)} \, , \qquad \frac{\partial^2 d_L(z)}{\partial z^2} = \frac{2H(z) - (1+z)H'(z)}{H(z)^2} \tag{61}$$

where $H'(z) = \frac{\dot{a}}{a_0} - \frac{\ddot{a}a}{a_0\dot{a}} = \frac{\dot{a}}{a_0}(1+q)$ and $q := -\frac{\ddot{a}a}{\dot{a}^2}$ is the deceleration parameter.
We use these two derivatives in the Taylor expansion:

$$d_L(z) = \frac{c}{H_0}\left[z + \frac{1-q_0}{2}z^2 + O\left(z^3\right)\right] \tag{62}$$

where we also reintroduced the speed of light $c$.
Figure 5 compares the analytical solution $d_L(z)$ (eq. 60) with the first and second order approximations (eq. 62). The vertical lines represent the maximum distance reached by E. Hubble in the discovery of the universe expansion [6] and by A.G Riess in the discovery of the acceleration of this expansion [10].

## 3.2 Early measurement

The cosmic microwave background (CMB) radiation was accidentally discovered by Arno Penzias and Robert Wilson in 1965 [14]. It is composed of an almost uniform and isotropic electromagnetic radiation that permeates all the space around us, its frequency spectrum corresponds to that emitted by a perfect black body at a temperature $T = (2.72548 \pm 0.00057)$K [9]:

$$I(\nu)\,\mathrm{d}\nu = \frac{2h\nu^3}{c^2(e^{\frac{h\nu}{kT}} - 1)}\,\mathrm{d}\nu \tag{63}$$

After its discovery, the CMB has been the subject of numerous studies and in 1992, in particular, a precise measurement of the temperature, as well as on the the anisotropic deviations from it was measured for the first time from space by COBE DMR instrument [15]. This anisotropy, as well as the polarization of the same radiation, has nowadays been measured with great precision by Planck satellite [7] and it is estimated to be of the order of $\delta T/T \sim 10^{-5}$. The statistics of these data have been and are being extensively studied to derive information regarding the geometry, composition, and initial conditions of the universe. In particular, it is used to estimate the six cosmological parameters such as the Hubble constant $H_0$. The last estimate is $H_0 = 67.4 \pm 0.5 \frac{\mathrm{km}}{\mathrm{sec\ Mpc}}$ [7].
Small variations in the CMB temperature across the sky, reflect spatial variations in the density of the primordial plasma, $\delta\rho_a := \rho_a - \overline{\rho}_a$, and related perturbations of the spacetime geometry, $\delta g_{\mu\nu} := g_{\mu\nu} - \overline{g}_{\mu\nu}$ (see previous section). This deviation from the homogeneous universe, that manifests itself at the time of recombination ($z \sim 1100$) at the order of $\delta T/T \sim 10^{-5}$, and which seeds the Large Scale Structures (LSS) that we can observe nowadays (with a significantly more pronounced density contrast), is believed to have originated during the inflationary period. According to the inflationary theories, the exponential growth of the scale factor during inflation caused quantum fluctuations of the inflaton field to be stretched to macroscopic scales, and to "freeze in" upon leaving the horizon (when $k \sim (aH)^{-1}$). As we also discussed in the previous section, these fluctuations re-enter inside the horizon in the following radiation and matter domination eras, and this sets the initial conditions for the anisotropies in the cosmic microwave background and for the distribution of matter in the universe. This concept is summarized in Figure 6.
Since the fluctuations are believed to arise from inflation, such measurements can also set constraints on parameters within inflationary theory.
In the next subsections we discuss the establishment of the CMB anisotropies, following refs. [11] and [18]. For simplicity, we consider a flat universe.

### 3.2.1 Anisotropy from inhomogeneity

Here we discuss how an inhomogeneity in the universe radiation density during recombination ($z \sim 1100$) leads to an anisotropy in the radiation that we measure nowadays from Earth ($z = 0$). Indeed, after electrons and protons recombination, the photons stop to scatter with them, and propagate almost freely until they reach our detectors. Therefore, it follows that an inhomogeneity (in the density and in the temperature) in the last scattering surface (the shell at the right distance from the Earth such that photons emitted at the time of decoupling are now received) causes the production of photons with energies different from the average, which propagate until they reach us. Variations of the

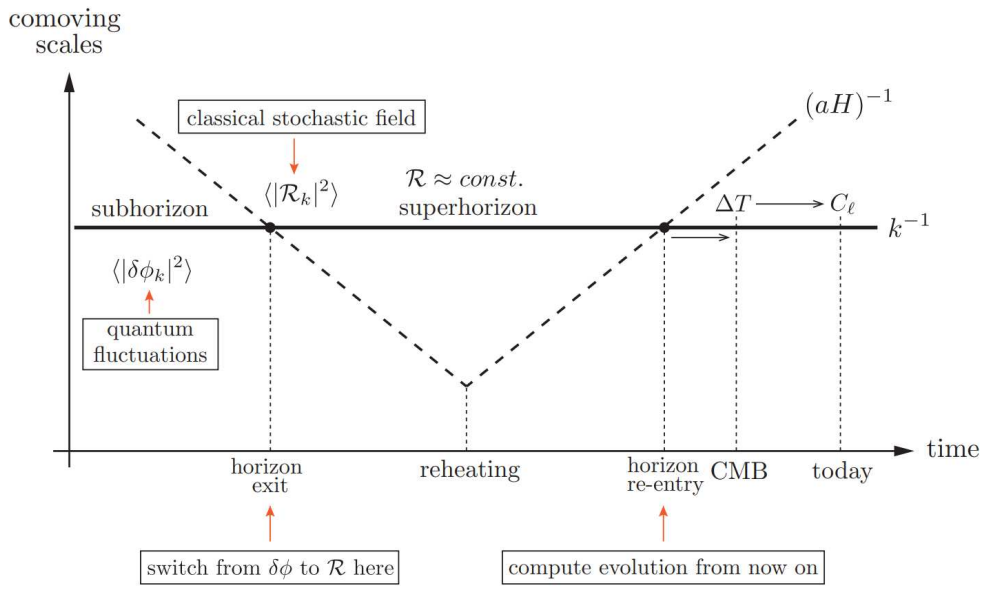


Figure 6: Evolution of perturbations (described by curvature perturbations) from their production during inflation to their detection today. Figure taken from ref. [3].

energy of the arrival photons can be also caused by time varying inhomogeneities of the geometry on which these photons propagate, through the so called integrated Sachs-Wolfe effect.
Before we start, it is important to stress that this whole process is stochastic. The perturbations are produced stochastically while sub-horizon during inflation (following a nearly Gaussian statistics with zero mean and scale-invariant variance). Therefore, although their subsequent evolution is a classical and deterministic process, the anisotropy of the CMB is a stochastic phenomenon. In other words, any physical information must be inferred from the statistical properties of the CMB temperature distribution. In particular, assuming the distribution to be Gaussian with zero mean, all its statistical information is contained in the two-point correlation function. This function quantifies the temperature correlation between any two-point in space. Assuming statistical homogeneity and isotropy, this correlation depends only on the distance between the two-point.
Let $T(\hat{\boldsymbol{n}})$ be the CMB temperature distribution measured from the direction $\hat{n}$ of our sky, and let $\overline{T}$ be its average over the whole celestial sphere. The quantity $\Theta(\hat{\boldsymbol{n}}) := (T(\hat{\boldsymbol{n}}) - \overline{T})/\overline{T}$ represents the anisotropy distribution, with vanshing mean. In this context a harmonic description is more efficient than a real space description, and the appropriate harmonics are the spherical harmonics (the eigenfunctions of the Laplace operator on the sphere that form a complete basis for scalar functions on it):

$$\Theta(\hat{\boldsymbol{n}}) = \sum_{lm} \Theta_{lm} Y_{lm}(\hat{\boldsymbol{n}}) \tag{64}$$

Given the definition of $\Theta(\hat{\boldsymbol{n}})$, we have that $\Theta_{00} = 0$.
Furthermore, for statistically isotropic fluctuations (i.e. $\langle\Theta(\hat{\boldsymbol{n}})\Theta(\hat{\boldsymbol{n}}')\rangle = f(\hat{\boldsymbol{n}} \cdot \hat{\boldsymbol{n}}')$), the ensemble average of the temperature fluctuation coefficients $\Theta_{lm}$ satisfies:

$$\langle\Theta^*_{lm}\Theta_{l'm'}\rangle = \delta_{ll'}\delta_{mm'}C_l \quad \Longrightarrow \quad C_l = \langle|\Theta_{lm}|^2\rangle = \frac{1}{2l+1}\sum_{m=-l}^{l}|\Theta_{lm}|^2 \tag{65}$$

with $C_l$ being the power spectrum coefficients.
If we temporarily disregard for simplicity the integrated Sachs-Wolfe effect, under the instantaneous recombination approximation, the angular temperature fluctuation distribution is simply a projection of the spatial temperature fluctuation in the last scattering surface at the recombination:

$$\Theta(\hat{\boldsymbol{n}}) = \int \mathrm{d}D\ \Theta(\boldsymbol{x})\delta(D - D_*) \tag{66}$$

where $D = \int \mathrm{d}z/H$ is the comoving metric distance, $D_*$ denotes the distance a CMB photon travels from recombination, and $\Theta(\boldsymbol{x}) := (T(\boldsymbol{x}) - \overline{T})/\overline{T}$ is the spatial temperature fluctuation at recombination. Note that the cosmological redshift does not appear in the temperature fluctuation since the background and fluctuation redshift alike.
We can decompose $\Theta(\boldsymbol{x})$ in Fourier modes as in eq. 49. Since $\Theta(\boldsymbol{x})$ fluctuations are statistically homogeneous and isotropic (i.e. $\langle\Theta(\boldsymbol{x})\Theta(\boldsymbol{x}')\rangle = f(|\boldsymbol{x} - \boldsymbol{x}'|)$), the two-point function of the Fourier coefficients $\Theta(\boldsymbol{k})$ is described by the power spectrum $P(k)$:

$$\langle\Theta(\boldsymbol{k})^*\Theta(\boldsymbol{k}')\rangle = (2\pi)^3\delta(\boldsymbol{k} - \boldsymbol{k}')P(\boldsymbol{k}) = (2\pi)^3\delta(\boldsymbol{k} - \boldsymbol{k}')P(k) \tag{67}$$

with $(2\pi)^3$ a normalization factor. Since $P(\boldsymbol{k}) = P(k)$:

$$\langle\Theta(\boldsymbol{x})\Theta(\boldsymbol{x})\rangle = \int \frac{\mathrm{d}^3k}{(2\pi)^3}P(k) = \int_0^\infty \mathrm{d}(\ln k)\,\frac{k^3P(k)}{2\pi^2} = \int_0^\infty \mathrm{d}(\ln k)\,\Delta^2_\Theta(k) \tag{68}$$

with $\Delta^2_\Theta(k) := k^3P(k)/(2\pi^2)$.
To relate this to the amplitude of the angular power spectrum, we have to expand equation 66 in Fourier modes. Therefore, applying the Dirac delta function:

$$\Theta(\hat{\boldsymbol{n}}) = \int \mathrm{d}D \int \frac{\mathrm{d}^3k}{(2\pi)^3}\Theta(\boldsymbol{k})e^{i\boldsymbol{k}\cdot(D\hat{\boldsymbol{n}})}\delta(D - D_*) = \int \frac{\mathrm{d}^3k}{(2\pi)^3}\Theta(\boldsymbol{k})e^{i\boldsymbol{k}\cdot(D_*\hat{\boldsymbol{n}})} \tag{69}$$

The Fourier modes themselves can be expanded in spherical harmonics with the relation:

$$e^{i\boldsymbol{k}\cdot(D_*\hat{\boldsymbol{n}})} = 4\pi\sum_{lm} i^l j_l(kD_*)Y^*_{lm}(\hat{\boldsymbol{k}})Y_{lm}(\hat{\boldsymbol{n}}) \tag{70}$$

where $j_l$ are the spherical Bessel functions (mentioned in the previous section). Extracting the multipole moments from eq. 69 and 70, we obtain:

$$\Theta_{lm} = \int \frac{\mathrm{d}^3k}{(2\pi)^3}\Theta(\boldsymbol{k})4\pi i^l j_l(kD_*)Y_{lm}(\hat{\boldsymbol{k}}) \tag{71}$$

Finally:

$$\langle\Theta^*_{lm}\Theta_{l'm'}\rangle = \delta_{ll'}\delta_{mm'}4\pi\int_0^\infty \mathrm{d}(\ln k)j_l^2(kD_*)\Delta^2_\Theta(k) \tag{72}$$

Assuming a slowly varying power spectrum $\Delta^2_\Theta(k)$ (as we will see better later) we can take it out of the integral and evaluate it at the peak of the Bessel function $kD_* \approx l$. The remaining integral gives $\int_0^\infty \mathrm{d}(\ln x)\; j_l^2(x) = [2l(l+1)]^{-1}$, hence:

$$C_l \approx \frac{2\pi}{l(l+1)}\Delta^2_\Theta(l/D_*) \tag{73}$$

Therefore, we have seen that it is possible to relate the $C_l$ coefficients (estimated from measurements of $T(\hat{\boldsymbol{n}})$ using equations 64 and 65) to the parameter $\Delta^2_\Theta(k)$ evaluated at the time of ricombination. The purpose of the next paragraphs will be to find how generic scale-invariant power spectrum of primordial curvature perturbations at the beginning of the universe $\zeta(\boldsymbol{k}, 0)$:

$$\Delta^2_\zeta(k) \sim const. \qquad \text{with} \quad \langle\zeta(\boldsymbol{k},0)^*\zeta(\boldsymbol{k}',0)\rangle = (2\pi)^3(2\pi^2/k^3)\delta(\boldsymbol{k} - \boldsymbol{k}')\Delta^2_\zeta(k) \tag{74}$$

turns into the power spectrum of temperature $\Delta^2_\Theta(k)$. In other words, we will find the classical and deterministic transfer function $T(k)$ such that:

$$\Theta(\boldsymbol{k}) = T(k)\,\zeta(\boldsymbol{k}) \quad \Longrightarrow \quad \Delta^2_\Theta(k) = T^2(k)\,\Delta^2_\zeta(k) \tag{75}$$

Indeed, as we said in the previous section, the statistics of the primordial adiabatic pertrubations is fully described by that of the curvature mode $\zeta$.
Finally, since the transfer function $T(k)$ depends on the behavior of the cosmological model from the end of inflation to the present time (and therefore on parameters such as $\Omega_m$, $\Omega_\Lambda$, ...), and since the power spectrum $\Delta_\zeta(k)$ depends on the inflationary model (and its related parameters), thus it is possible to test a generic cosmological theory (such as the standard $\Lambda$CDM model) and determine its parameters by fitting the power spectrum $C_l$ obtained from the cosmic microwave background radiation. The fit of the $\Lambda$CDM model performed by Planck collaboration is shown in Figure 7.

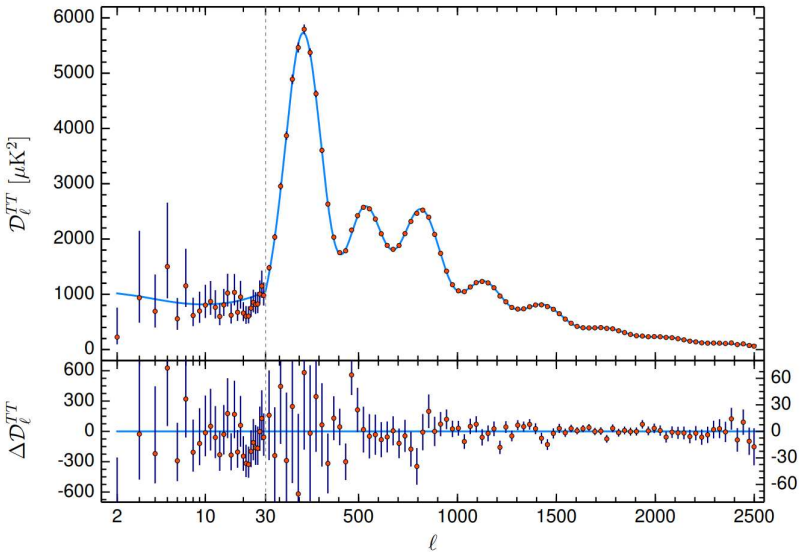


Figure 7: Temperature power spectrum (temperature-temperature correlation) from recent measurements from Planck mission. $D_l := [l(l+1)/(2\pi)]\, C_l$ where $C_l$ is the one defined in this dissertation multiplied by the square of the background temperature today $\overline{T}$. The base ΛCDM theoretical spectrum best fit is plotted in light blue in the upper panel. Figure taken from ref. [7].

### 3.2.2 Transfer function

The cosmological principle of statistical isotropy refers to one specific frame, which we denote as CMB rest-frame. Violation of isotropy is observed in any other frame. The largest anisotropy measures in the CMB is actually not of cosmological origin, but it is due to the peculiar motion of the solar system in the CMB rest-frame. Consider a photon entering our detectors from a direction $\hat{\boldsymbol{n}}$. In the rest frame of the CMB it has momentum $\boldsymbol{p} = -p\hat{\boldsymbol{n}}$. Due to the relativistic Doppler effect, the observed momentum is:

$$p_{obs}(\hat{\boldsymbol{n}}) = \frac{p}{\gamma(1-\hat{\boldsymbol{n}}\cdot\boldsymbol{v})} = p\left(1+\hat{\boldsymbol{n}}\cdot\boldsymbol{v}+O\left(v^2\right)\right) \qquad \text{since} \quad p=(2\pi)\nu \tag{76}$$

with $\boldsymbol{v}$ the Solar System velocity relative to the CMB rest frame such that $|\boldsymbol{v}| \ll 1$ ($v \sim 370$ km/s [16]). Since the CMB has a blackbody spectrum, we can relate the change in the observed momentum of photons to a change in the observed temperature (using that $\nu_{peak} \propto T$):

$$\Theta_{Dop}(\hat{\boldsymbol{n}}) = \frac{T_{obs}(\hat{\boldsymbol{n}})-\overline{T}}{\overline{T}} = \frac{p_{obs}(\hat{\boldsymbol{n}})-\overline{p}}{\overline{p}} = \hat{\boldsymbol{n}}\cdot\boldsymbol{v} = v\cos\theta \tag{77}$$

up to $O\left(v^2\right)$ terms that we disregard. Therefore, to leading order in $v$, the Doppler effect contributes only to the coefficient of the spherical harmonic $Y_{10} = \sqrt{\frac{3}{4\pi}}\cos(\theta)$ : $\Theta_{10}^{Dop} = \sqrt{\frac{4\pi}{3}}v$, where we have directed the $z-$axis along the direction of $\boldsymbol{v}$. Hence, it only impacts the value of $C_1$, which was excluded from the fit in Figure 7.

Let us trace the life of a photon ($X^\mu(\lambda)$) after decoupling. In doing so, we now include also the integred Sachs-Wolfe effect that we disregarded in the above discussion. In the absence of additional non-gravitational forces, freely-falling particle (massive or massless) in a curved spacetime moves along geodesics:

$$P^\nu\nabla_\nu P^\mu = P^\nu\left(\frac{\partial P^\mu}{\partial x^\nu}+\Gamma^\mu_{\nu\rho}P^\rho\right) = 0 \tag{78}$$

with $P^\mu$ the four-momentum of the particle. In particular, this equation for massive particles can be obtained extremizing the action of a free particle in a curved spacetime (see [3]):

$$S[X^\mu(\lambda)] = -m\int_A^B \mathrm{d}s = -m\int_{\lambda_A}^{\lambda_B}\sqrt{g_{\mu\nu}(X)\dot{X}^\mu\dot{X}^\nu}d\lambda \tag{79}$$

while the massless case coincides with the $m \to 0$ limit of the massive particle case.
If we initially consider only the flat background metric in the calculation of the Christoffel symbols, then we obtain (since $\partial_i P^\mu = 0$):

$$P^0 \frac{\mathrm{d}P^\mu}{\mathrm{d}t} = -\Gamma^\mu_{\alpha\beta} P^\alpha P^\beta \quad \Longrightarrow \quad p \propto \frac{1}{a} \tag{80}$$

with $p$ the momentum of the particle ($p = E$ for massless particle and $p = \gamma m v$ for massive particle). Since the effect of the background metric acts identically on both $p_{obs}(\hat{\boldsymbol{n}})$ and $\overline{p}$, the observable $\Theta(\hat{\boldsymbol{n}})$ is not influenced by the expansion of the universe that occurs during the photon trajectory. At this point it is necessary to calculate the geodesic equation in the inhomogeneous universe to first order in perturbation theory. Using conformal time and the Newton gauge, defined in the previous section, we obtain (see [11]):

$$\frac{\mathrm{d}}{\mathrm{d}\tau} \ln(ap) = -\frac{\mathrm{d}\Psi}{\mathrm{d}\tau} + \frac{\partial(\Psi + \Phi)}{\partial\tau} \tag{81}$$

where $\frac{\mathrm{d}}{\mathrm{d}\tau}$ represents the total derivative of $\ln(a(\tau)p(\tau))$ and $\Psi(\tau, X^i(\tau))$ with respect to conformal time, while $\frac{\partial}{\partial\tau}$ represents the partial derivative of $(\Psi + \Phi)$ with respect to conformal time.
In the absence of the source terms on the right hand side, this implies $p \propto a^{-1}$. The inhomogeneous source terms describe how photons lose or gain energy as they move out of or into potential wells. Working in the idealised approximation of instantaneous recombination (at conformal time $\tau_*$ of last scattering), we can integrate the geodesic equation along a line of sight and so relate the observed CMB temperature anisotropies (at conformal time $\tau_0$) to the fluctuations at recombination:

$$\ln(ap)_0 = \ln(ap)_* + (\Psi_* - \Psi_0) + \int_{\tau_*}^{\tau_0} \mathrm{d}\tau \, \frac{\partial}{\partial\tau}(\Psi + \Phi) \tag{82}$$

Using that $ap \propto a\overline{T}(1 + \Theta)$, $a_0\overline{T}_0 = a_*\overline{T}_*$ and Taylor-expanding the logarithms to first order in $\Theta$, we find:

$$\Theta_0 = \Theta_* + (\Psi_* - \Psi_0) + \int_{\tau_*}^{\tau_0} \mathrm{d}\tau \, \frac{\partial}{\partial\tau}(\Psi + \Phi) \tag{83}$$

The term $\Phi_0$ only affects the monopole perturbation, so it is unobservable and therefore dropped from the equation. Moreover, the fractional temperature perturbation at last scattering can be expressed in terms of the density contrast of photons, $\delta_\gamma := (\rho_\gamma - \overline{\rho}_\gamma)/\overline{\rho}_\gamma$, as:

$$\Theta_* = \frac{1}{4}(\delta_\gamma)_* \tag{84}$$

since $\rho_\gamma \propto T^4$, as we showed in eq. 12. Hence:

$$\Theta_0 = (\frac{1}{4}\delta_\gamma + \Psi)_* + \int_{\tau_*}^{\tau_0} \mathrm{d}\tau \, \frac{\partial}{\partial\tau}(\Psi + \Phi) \tag{85}$$

So far, we have ignored the motion of the electrons at the surface of last scattering, the inclusion of which leads to:

$$\Theta(\hat{\boldsymbol{n}}) = \left(\frac{1}{4}\delta_\gamma + \Psi + \hat{\boldsymbol{n}} \cdot \boldsymbol{v}_e\right)_* + \int_{\tau_*}^{\tau_0} \mathrm{d}\tau \, (\Psi' + \Phi') \tag{86}$$

with $\boldsymbol{v}_e$ the electrons velocity at the time of the last scattering surface (LSS) measured in the rest frame of the observer.
Each term on the right hand side has the following physical interpretation:

- the term $\frac{1}{4}\delta_\gamma$ is the intrinsic temperature variation over the background LSS;
- the term $\Psi$ arises from the gravitational redshift that the photons experience when climbing out of a potential well at last scattering. The combination $(\frac{1}{4}\delta_\gamma + \Psi)$ is often called the Sachs-Wolfe (SW) term;
- the $\hat{\boldsymbol{n}} \cdot \boldsymbol{v}_e$ is the Doppler effect due to the electrons motion at the LSS;

- finally, the $\int \mathrm{d}\tau\ (\Psi' + \Phi')$ term is called integrated Sachs-Wolfe (ISW) term and describes the effect of gravitational redshifting from evolution of the potentials along the line of sight between $\tau_*$ and $\tau_0$. During matter domination era $\Psi' \approx \Phi' \approx 0$ (as we showed in eq. 35 and 57) and this term vanishes.

Figure 8 illustrates the contributions that each of the terms in eq. 86 makes to the power spectrum of the CMB temperature anisotropies. We see that the integrated Sachs-Wolfe (ISW) contribution is subdominant. For this reason we will neglect it in the following discussion.

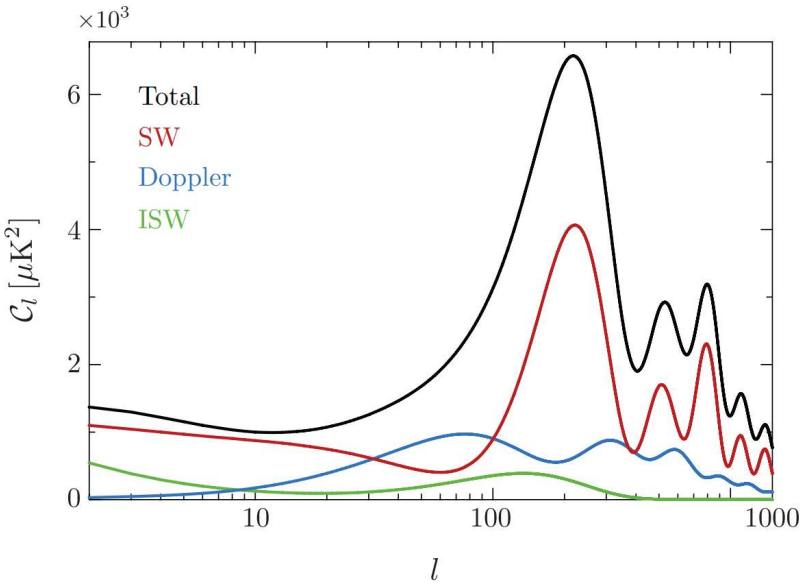


Figure 8: Contributions of the various terms in eq. 86 to the power spectrum of CMB anisotropies. Figure taken from ref. [11].

The equation 86 highlights terms that we had not specified or that we had ignored in determining the expression for $C_l$ factors (eq. 73). Therefore, if we proceed with the generalization:

$$\Theta(\boldsymbol{x}, \tau_*) \quad \longrightarrow \quad \left(\frac{1}{4}\delta_\gamma + \Psi + \hat{\boldsymbol{n}} \cdot \boldsymbol{v}_e\right)_* \tag{87}$$

where we have neglected the ISW term, the formula for the $C_l$ factors (without going into the details of the proof) changes as follows [19]:

$$C_L = 4\pi \int_0^\infty \mathrm{d}(\ln k) j_l^2(kD_*)\Delta_\Theta^2(k) \quad \longrightarrow \quad C_L = 4\pi \int_0^\infty \mathrm{d}(\ln k) T_l^2(k)\Delta_\zeta^2(k) \tag{88}$$

$$\text{with:} \qquad T_l(k) := T_{SW}(k) j_l(kD_*) + T_D(k) j_l'(kD_*)\ , \quad T_{SW} := \frac{(\frac{1}{4}\delta_\gamma + \Psi)_*}{\zeta(\boldsymbol{k}, \tau_{\text{in}})}\ , \quad T_D := -\frac{(v_e)_*}{\zeta(\boldsymbol{k}, \tau_{\text{in}})} \tag{89}$$

where $T_{SW}(k)$ and $T_D(k)$ are the transfer functions that defines how the curvature perturbation ($\zeta$) at time $\tau = \tau_{\text{in}}$ evolve into density, gravitational and velocity perturbations ($\delta_\gamma$, $\Phi$, $v_e$) at the time of recombination $\tau_*$.
Finally, since both the Bessel function $j_l(kD_*)$ and its derivative $j_l'(kD_*)$ act almost like delta functions and map the Fourier modes $k$ to the harmonic moments $l \sim kD_*$, we can find the generalization of eq. 73:

$$C_l \approx \frac{2\pi}{l(l+1)} \left[T_{SW}^2(k) + T_D^2(k)\right] \Delta_\zeta^2(k)\Big|_{k \sim l/D_*} \tag{90}$$

where we have dropped the cross term $T_{SW}(k)T_D(k)$ because it is negligible.
Without going into detail about inflation theories, they predict the shape of the curvature perturbations power spectrum $\Delta_\zeta^2(k)$ (for more details see [2] or [11]):

$$\Delta_\zeta^2(k) = A_s \left(\frac{k}{k_*}\right)^{n_s - 1} \qquad \text{with} \quad k_* := -\frac{1}{\tau_*} \tag{91}$$

where $A_s$ is called curvature fluctuation amplitude and $n_s$ scalar spectral index. Given that recent measurements have estimated $n_s = 0.965 \pm 0.004$ [7], we can state that the scale invariance approximation $\Delta^2_\zeta(k) \sim const.$ is verified. Therefore, the only quantities in equation 90 that significantly modulate the $C_l$ factors are the transfer function $T_{SW}$ and $T_D$. In the next section, we will discuss the evolution effects that determine the dominant transfer function $T_{SW}$ and hence the CMB power spectrum.

### 3.2.3 Cosmic sound waves and imprints in the CMB

As the inflaton decays and reheats the universe, the inflaton primordial perturbations ($\delta\phi$) turn into matter and radiation perturbations ($\delta T^{\mu\nu}_\gamma$, $\delta T^{\mu\nu}_{\text{baryons}}$, ...). The latter, along with the corresponding metric perturbations ($\delta g_{\mu\nu}$), remain frozen until the horizon crossing, when the interactions between photons and matter result in oscillatory amplitudes of the perturbations, known as baryon acoustic oscillations (BAO). In the early universe, electrons and baryons (mostly protons) are strong coupled to each other via Coulomb scattering, at the same time electrons and photons interact via Thomson scattering. Hence the baryon acoustic oscillations are fluctuations in the density of the electron-baryon fluid caused by acoustic density waves. This tight coupling persists until recombination (at redshift $z \sim 1100$, during the matter dominated era), when free electrons and protons combine into neutral hydrogen, and photons start to stream freely.
Figure 9 shows how different scales of primordial perturbations influence the CMB temperature power spectrum.

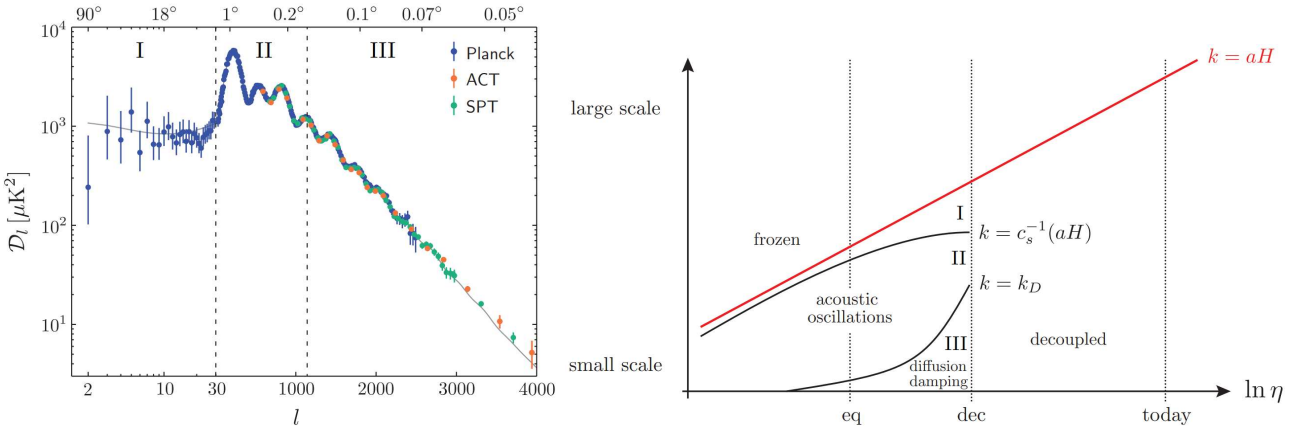


Figure 9: Effect of different scales of primordial perturbations on the CMB temperature power spectrum. Figure taken from ref. [19].

Perturbations on too large scales ($k < c_s^{-1}(aH)\big|_*$, where $c_s$ is the sound speed of the photon-baryon fluid that we define in this subsection) remain frozen until shortly before recombination, and therefore do not have enough time to perform BAO, resulting in a nearly constant power spectrum (zone I). Perturbations on intermediate scales ($c_s^{-1}(aH)\big|_* < k < k_D\big|_*$, with $k_D$ a characteristic damping scale) instead develop BAO and generate a spectrum with oscillations (zone II). Fnally, modes that correspond so scales smaller than the photon mean free path ($k > k_D\big|_*$) are strongly damped by the photon diffusion (this is known as Silk damping [24]). This leads to an exponential decay of the power spectrum (zone III). In particular, the effect of exponential damping can be represented as [19]: $T(k) \longrightarrow e^{-k^2/k_D^2} T(k)$ with $k_D = 2\pi/\lambda_D$, $\lambda_D = \sqrt{\tau \lambda_C}$, $\lambda_C = (n_e \sigma_T a)^{-1}$ where $n_e$ is the electron density and $\sigma_T$ is the Thomson cross section. The quantity $\lambda_C$ is the comoving mean free path, and $\lambda_D$ is the comoving diffusion length in the time $\tau$.
If our task is to compute the transfer functions $T_{SW}(k)$ and $T_D(k)$ in eq. 89, this requires us to solve the coupled fluctuation equations of photons, electrons, baryons and dark matter in a perturbed spacetime (dark energy is negligible at those times).
In this subsection we examine the physical processes involved in the formation of the acoustic peaks and we explain their sensitivity to the six parameters of the ΛCDM model (universe energy content, expansion rate, ...). Our treatment will be approximate and qualitative (further details can be found

in [19]).
By combining the continuity equation and the Navier-Stokes equation for photons, in particular substituting the divergence of equation 34 into the derivative (with respect to conformal time) of equation 33 using $\delta P/\delta\rho = \bar{P}/\bar{\rho} = 1/3$, we obtain:

$$\delta_\gamma'' - \frac{1}{3}\nabla^2\delta_\gamma = \frac{4}{3}\nabla^2\Psi + 4\Phi'' \tag{92}$$

This equation is valid only during the radiation domination era, when $\delta P/\delta\rho = \bar{P}/\bar{\rho} = 1/3$. If we take into account the interaction between photons and baryons during the early phase of the matter domination era, this equation generalizes to [19]:

$$\delta_\gamma'' + \frac{\mathcal{H}R}{1+R}\delta_\gamma' - c_s^2\nabla^2\delta_\gamma = \frac{4}{3}\nabla^2\Psi + 4\Phi'' + \frac{4\mathcal{H}R}{1+R}\Phi' \tag{93}$$

with:

$$c_s^2 := \frac{1}{3(1+R)} \quad , \qquad R := \frac{3}{4}\frac{\bar{\rho}_b}{\bar{\rho}_\gamma} \approx 0.6\left(\frac{\Omega_b h^2}{0.02}\right)\left(\frac{a}{10^{-3}}\right) \tag{94}$$

where $R$ is the ratio of the momentum densities of baryons and photons, while $c_s$ is the sound speed of the photon-baryon fluid. In the last relation, the scale factor is normalized to one today. Eq. 93 is a key relation for the CMB phenomenology. The various terms in this euqation have the following intepretation: $\delta_\gamma'$ is a "friction" term due to the expansion of the universe; $\nabla^2\delta_\gamma$ is the pressure term; $\nabla^2\Psi$ is the gravity term; finally, $\Phi''$, $\Phi'$ arise from time dilatation [11].
In practice, the equations describing the many coupled fluctuations in the primordial plasma have to be solved numerically. Anyway we can solve equation 93 by making several (more or less justified) approximations. Our goal is to understand the main features of the CMB power spectrum.
Defining $\Theta := \frac{1}{4}\delta_\gamma + \Psi$ (following the previous chapter convention), considering $\Psi \approx \Phi$ (valid in absence of anisotropic stress $\Pi$), neglecting the time dilation terms $\Phi'$, $\Phi''$, and imposing $\rho_\gamma \gg \rho_b \implies R \ll 1$ (true during radiation domination era), the equation 93 simplifies significantly:

$$\ddot{\Theta} - c_s^2\nabla^2\Theta = 0 \tag{95}$$

where the solutions in the Fourier space are:

$$\Theta(\boldsymbol{k}, \tau) = A_{\boldsymbol{k}}\cos(c_s k\tau) + B_{\boldsymbol{k}}\sin(c_s k\tau) \tag{96}$$

imposing the initial conditions in terms of the curvature perturbation [19], we obtain:

$$\Theta(\boldsymbol{k}, \tau) = 3\zeta_{\boldsymbol{k}}\cos(c_s k\tau) \tag{97}$$

where we have approximated the conformal time at the horizon crossing equal to zero $\tau_{\text{hc}} \sim 0$ (valid for sufficiently small wavelengths). It follows, by definition 89, that:

$$T_{SW}(k) = \frac{\Theta(\boldsymbol{k}, \tau_*)}{\zeta_{\boldsymbol{k}}} = 3\cos(c_s k\tau_*) \tag{98}$$

Since the CMB power spectrum is proportional to the square of the transfer function, its peaks occur at multiples of a fundamental scale $k_n = nk_*$ with $n \in \mathbb{N}$, $k_* := \pi/s_*$ and $s_* := c_s\tau_* \sim \tau_*/\sqrt{3}$ (the sound horizon at recombination). Reminding that in eq. 90 the transfer function is evaluated in $k \sim l/D_*$, the fundamental scale $k_*$ becomes a characteristic angular scale by simple projection: $l_* = k_* D_* \sim 2\pi\tau_0/\tau_*$, where $D_* = \tau_0 - \tau_* \sim \tau_0$ (in a flat universe). Assuming a purely matter dominated universe after recombination, we have $\tau \propto a^{1/2}$ and therefore we find:

$$l_* \sim 2\pi\left(\frac{\tau_0}{\tau_*}\right) \sim 2\pi\left(\frac{a_0}{a_*}\right)^{1/2} \sim 2\pi\left(\frac{z_*}{z_0}\right)^{1/2} \sim 2\pi\left(\frac{1100}{1}\right)^{1/2} \sim 200 \qquad \longrightarrow \qquad \theta_* := \frac{2\pi}{l_*} \sim 2^\circ \tag{99}$$

It is important to note how this value $l_*$ coincides with the value of $l$ corresponding to the first peak in Figure 7. Therefore, with this simplified treatment, we manage to determine the fundamental angular

scale of the power spectrum. However, this result is based on the assumptions that dark energy is negligible and that the universe is flat. Angular distances (as $D_*$ in $\theta_* = s_*/D_*$) are indeed very sensitive to the current dark energy component $\rho_\Lambda(t_0)$ and to the geometry of the universe $k$. In fact $d_A = d_m/(1+z) = a_0 S_k(\chi)/(1+z)$ with $S_k(\chi)$ (defined in eq. 2) depending on $k$, in particular $S_k(\chi)$ increases as $k$ decreases ($R\sin(x/R) < \sin x < x < \sinh x < R\sinh(x/R)$ for $x \ll 1$ and $0 < R < 1$ the curvature radius). Moreover $S_k(\chi)$ increases also when $\chi$ increases and, in the flat universe approximation, eq. 59 leads to $\chi = a_0^{-1}\int_0^z \mathrm{d}\tilde{z}/H(\tilde{z})$. Therefore the angular distance is sensible to the duration of the period (in terms of red-shift $z$) where the value of $H^{-1}$ is big, and so the duration of the recently dark energy dominated era (the Hubble parameter decreases during matter and radiation eras and is constant during dark energy era). Hence increasing the value of $\rho_\Lambda(t_0)$ increases the duration of dark energy dominated era and so the Hubble parameter $H(z)$ stops decreasing sooner, this implies that the value of $\chi$ and the angular distance decrease. Since $l_* = 2\pi/\theta_* = (2\pi D_*)/s_*$, it follows that the power spectrum shifts on left as $k$ or $\rho_\Lambda(t_0)$ increases. These considerations can be compared and verified with the simulations in the two top figures of Table 1. It is this dependence between angular distance and these two parameters that allows us to extract the values of the dimensionless current time parameters $\Omega_k h^2 \propto -k = \Omega_k(a_0^2 H_0^2)$ and $\Omega_\Lambda h^2 \propto \rho_\Lambda = \Omega_\Lambda \frac{3H_0^2}{8\pi G}$, with $h := H_0/(100\frac{\mathrm{km}}{\mathrm{sec\ Mpc}})$.

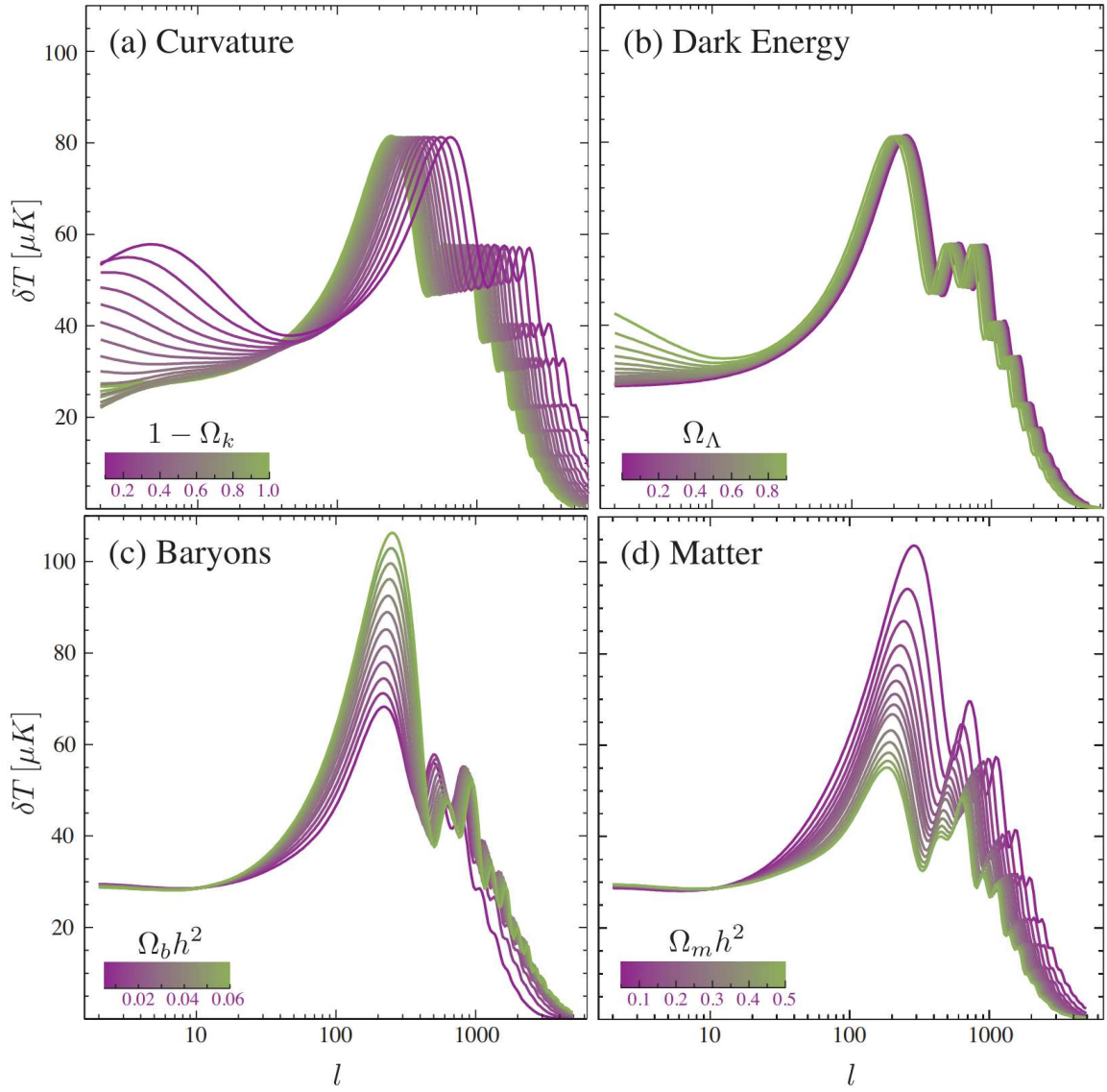


Table 1: The CMB power spectrum as a function of the following cosmological parameters: $\Omega_k$, $\Omega_\Lambda$, $\Omega_b h^2$, $\Omega_m h^2$. Figure taken from ref. [19].

As mentioned, the simplified treatment discussed so far neglects the energy density of baryons. In reality, before recombination, the universe undergoes the radiation-matter equality where the value of

$R$ increases until it can no longer be neglected (since baryons constitute a non-negligible fraction of the matter energy density):

$$R := \frac{3}{4}\frac{\overline{\rho}_b}{\overline{\rho}_\gamma} \propto a \quad \Longrightarrow \quad R(\tau) = \frac{3}{4}\frac{\Omega_b}{\Omega_m}\frac{a(\tau)}{a(\tau_{\rm eq})} \quad \Longrightarrow \quad R(\tau_*) \sim 0.15\frac{3}{4}\frac{a(\tau_*)}{a(\tau_{\rm eq})} \sim 0.15\frac{3}{4}\frac{z_{\rm eq}}{z_*} \sim 0.35 \tag{100}$$

If we now consider the same assumptions that lead equation 93 to the form 95 but this time neglecting the friction term $\delta'_\gamma$, assuming $R \sim 1$, and using $4/3 = 4c_s^2(1+R)$, equation 93 becomes:

$$\frac{\mathrm{d}^2}{\mathrm{d}\tau^2}(\Theta + R\Psi) - c_s^2\nabla^2(\Theta + R\Psi) = 0 \tag{101}$$

which improves over eq. 95. Following the same steps lading from eq. 95 to its solution, eq. 97, the "improved" eq. 101 is solved by:

$$\Theta(k,\tau) = 3\zeta_k\cos(c_s k\tau) - R\Psi(k) \quad \Longrightarrow \quad T_{SW}(k) = 3\cos(c_s k\tau_*) - \frac{R\Psi(k)}{\zeta_k} \tag{102}$$

Since the CMB power spectrum is proportional to the square of the transfer function, the negative shift of the $\Theta$ function solution caused by baryons leads to odd and even peaks in the CMB having unequal heights, in particular it increases the odd peaks (for which the cosine assumes the minimum value $-1$), while it increases the even peaks (for which the cosine assumes the maximum value $+1$), see Figure 10. The effect of the presence of baryons can be visualized in the bottom left figure of Table 1. The relative heights of the CMB spectrum therefore provide a measure of the baryon density $\Omega_b h^2$.

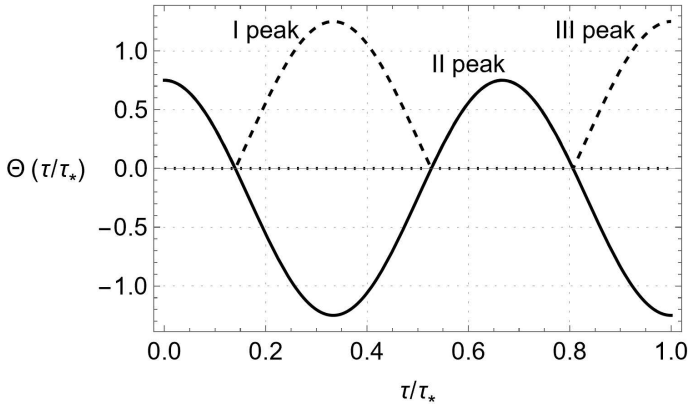


Figure 10: Acoustic oscillations with baryons. Solution of eq. 101 with $k = k_3 = 3k_*$, $\Psi(k) > 0$ and $\zeta_k > 0$ (solid line), and its absolute value (dashed line).

Now, let us discuss the effect of the terms proportional to time derivatives of the gravitational potential $\Phi \approx \Psi$ that we have neglected above. The gravitational potential oscillates inside the horizon during the radiation dominated era, generating a "driving force" in eq. 93. This enhances the amplitude of the combination $\Theta$ for the modes that entered the horizon during the radiation dominated era (typically $l \gtrsim 100$). This enhancement is strongest at matter-radiation equality [19]. Decreasing the matter density shifts equality to later times, placing it closer to recombination, therefore resulting in a greater enhancement. This is visible in bottom left panel of Table 1. From this effect, we can derive the ratio between the matter and radiation energy densities, and therefore, the present value of the matter density of the universe $\Omega_m h^2$ (as $\Omega_\gamma h^2$ is fixed by the observed CMB temperature [9]).
Naturally, the CMB power spectrum depends on the initial conditions at the end of inflation $\tau_{\rm in}$ (see eq. 90). Therefore, if we assume the standard inflation scenario characterized by a single scalar field, and thus we assume that the curvature perturbations power spectrum $\Delta^2_\zeta(k)$ takes the form in eq. 91, then fitting the CMB data can obviously determine the values of the curvature fluctuation amplitude $A_s$ and scalar spectral index $n_s$.
Finally, regarding the Hubble constant, above we saw that the last scattering surface angular distance $D_*$ is proportional to $h^{-1}$, indeed $D_* \propto \int_0^z \mathrm{d}\tilde{z}/H(\tilde{z}) \propto h^{-1}$. It is also possible to show that the ratio

$\theta_* = s_*/D_*$ can be well fit by a function of $\Omega_m h^3$ [23] (see also [22]). This can be combined with the value of $\Omega_m h^2$, determined by the height of the peaks discussed above, to give the value of $h$, namely the Hubble constant $H_0$.

# 4 Conclusion

The Hubble constant is a fundamental cosmological parameter that quantifies the current rate of expansion of the universe. It describes how quickly galaxies are moving away from each other due to the expansion of the universe (namely, at the net of their peculiar motion). In this thesis, we have reviewed the theoretical framework underlying the two currently most prominent methods to measure the Hubble constant. These two methods are called "local" and "global", since they rely, respectively, on the measurements of events in the late universe, and the measurement of the CMB, that is sensitive to the full cosmological evolution.

To review the theory underlying the two methods, we discussed basic notions of the standard cosmological model. We first investigated the evolution of the universe under the approximation of homogeneity and isotropy (the so called cosmological principle, which appears to be well respected on average at large scales), solving the Einstein equations in the three different stages experienced by the universe (radiation, matter, and dark energy domination). Then, we introduced the cosmological perturbations theory, focusing on first order scalar perturbations and determining the equations for the evolution of the perturbative parameters of metric and matter (in Newtonian gauge). Finally, we saw how these perturbations manifest themselves at the end of inflation assuming a standard inflation scenario generated by a single scalar field.

Regarding the local measurement, we examined how the luminosity distance of an astronomical event is related to the redshift we observe and how the Hubble constant can be extracted from the Hubble diagram. Concerning the global measurement, we discussed how CMB anisotropies arise from inhomogeneities in the universe at the time of recombination, how to extract statistical information from the CMB data to the temperature power spectrum, and how this spectrum depends on both the shape of the initial perturbations at the end of inflation and their propagation (represented by the transfer function) within a perturbed universe. Subsequently, we derived the various terms characterizing the transfer function and we examined, at a qualitative and approximate level, how the cosmological parameters value (including the Hubble constant) influences the transfer function and hence the CMB power spectrum, demonstrating that a fit of the latter can determine the six free parameters of the $\Lambda$CDM model.

Currently, the two methods provide results that disagree with each other at about the $5\sigma$ level. This Hubble tension is one of the main open problems in current cosmology. This makes it a central topic in the current scientific debate, both to search for possible systematic errors in the two measurements (particularly, in the local one [25]) and to deepen our knowledge in possible new physics explanation that might modify the current standard cosmological model [1].

## References


[1] Di Valentino E., Riess A.G. et al. *In the Realm of the Hubble Tension: A Review of Solutions*. 2020. https://arxiv.org/abs/2103.01183

[2] Riotto A. *Inflation and the Theory of Cosmological Perturbations*. 2002. https://arxiv.org/abs/hep-ph/0210162

[3] Baumann D. *Cosmology, Part III Mathematical Tripos*. 2015. http://cosmology.amsterdam

[4] Liddle A.R. *An Introduction to Modern Cosmology*, Wiley. 2015

[5] Kolb E.W., Turner M. S. *The Early Universe*, CRC Press. 1994

[6] Hubble E. *A Relation Between Distance And Radial Velocity Among Extra-Galactic Nebulae*. 1929. https://www.pnas.org/doi/pdf/10.1073/pnas.15.3.168

[7] Planck Collaboration *Planck 2018 results. VI. Cosmological parameters*. 2021. https://arxiv.org/abs/1807.06209

[8] Riess A.G. et al. *Cosmic Distances Calibrated to 1% Precision with Gaia EDR3 Parallaxes and Hubble Space Telescope Photometry of 75 Milky Way Cepheids Confirm Tension with LambdaCDM*. 2020. https://arxiv.org/abs/2012.08534

[9] Fixsen D.J. *The Temperature of the Cosmic Microwave Background*. 2009. https://arxiv.org/abs/0911.1955

[10] Riess A.G. et al. *Observational Evidence from Supernovae for an Accelerating Universe and a Cosmological Constant*. 1998. https://arxiv.org/abs/astro-ph/9805201

[11] Baumann D. *TASI Lectures on Primordial Cosmology*. 2018. https://arxiv.org/abs/1807.03098

[12] Bardeen J.M. *Gauge Invariant Cosmological Perturbations*. 1980. https://inspirehep.net/literature/159548

[13] Hu J., Wang F. *Hubble Tension: The Evidence of New Physics*. 2023. https://arxiv.org/abs/2302.05709

[14] Penzias A., Wilson R. *A Measurement of Excess Antenna Temperature at 4080 Mc/s*. 1965 https://ui.adsabs.harvard.edu/link_gateway/1965ApJ...142..419P/ADS_PDF

[15] Smoot G.F. et al. *Structure in the COBE Differential Microwave Radiometer First-Year Maps*. 1992. https://ui.adsabs.harvard.edu/link_gateway/1992ApJ...396L...1S/ADS_PDF

[16] Gordon C. et al. *Determining the motion of the solar system relative to the cosmic microwave background using type Ia supernovae*. 2007. https://arxiv.org/pdf/0711.4196

[17] Kurki-Suonio H. *Cosmological Perturbation Theory I*. 2022. http://www.courses.physics.helsinki.fi/teor/cpt/CosPer.pdf

[18] Hu J. *Lecture Notes on CMB Theory: From Nucleosynthesis to Recombination*. 2008. https://arxiv.org/pdf/0802.3688

[19] Baumann D. *Advanced Cosmology*. 2016. http://cosmology.amsterdam

[20] Perlmutte S. et al. *Measurements of* $\Omega$ *and* $\Lambda$ *from 42 high redshift supernovae*. 1998. https://arxiv.org/pdf/astro-ph/9812133

[21] Dalang C., Bonvin C. *On the kinematic cosmic dipole tension*. 2022. https://arxiv.org/pdf/2111.03616

[22] Wands D. et al. *Physics of the Cosmic Microwave Background Radiation*. 2015. https://arxiv.org/pdf/1504.06335

[23] Mukhanov V. *Physical foundations of cosmology*. 2005

[24] Silk J. *Cosmic Black-Body Radiation and Galaxy Formation.* 1968. https://ui.adsabs.harvard.edu/abs/1968ApJ...151..459S/abstract

[25] Riess A.G. et al. *Crowded No More: The Accuracy of the Hubble Constant Tested with High Resolution Observations of Cepheids by JWST.* 2023. https://arxiv.org/abs/2307.15806